UNIVERSITY OF GHANA

COLLEGE OF BASIC AND APPLIED SCIENCES

DEPARTMENT OF EARTH SCIENCE

AMBIENT NOISE H/V SPECTRAL RATIO FOR SITE EFFECT ESTIMATION IN SOME PARTS OF THE GREATER ACCRA REGION, GHANA.

BY

OWUSU-APPIAH, CHRISTIAN

10877244

THIS THESIS IS SUBMITTED TO UNIVERSITY OF GHANA, LEGON, IN PARTIAL FULFILLMENT OF THE REQUIREMENT FOR THE AWARD OF MPHIL APPLIED GEOPHYSICS DEGREE

DECEMBER, 2023

DECLARATION

I, Christian Owusu-Appiah, hereby declare that this is a result of original research undertaken under the guidance of Dr. T.E.K. Armah and Dr. E. A. Dzikunoo toward the Master of Philosophy degree in Geophysics in the Earth Science Department, University of Ghana. It is devoid of previously published materials by another individual(s), nor does it contain any materials that have been approved for the honour of any other degree at this University or elsewhere, to the best of my knowledge. All references to the work of other researchers and organizations have been duly acknowledged.

…… ……..13/12/2023…….……

Christian Owusu-Appiah (Student) Date

……..13/12/2023…….……

…… Date

Dr T. E. K. Armah (Principal Supervisor)

…… ……13/12/2023……..…

Date

Dr E. A. Dzikunoo (Co-Supervisor)

ABSTRACT

The soils in the Greater Accra Metropolitan Area (GAMA) soils have complex lithologies with varying spatial distribution mainly owing to bedrock, drainage, and topography. They are characterized by silty-sandy clays, heavy clays, and fine to coarse sand mostly in lower elevations, which grade to a range of gravely or highly quarzitic cobbly lateritic soils on higher grounds. The region is active seismically and has a history of earthquakes with destructive intensities occurring both recently and in the past. The recent surge in urbanization has made it possible to analyze and understand site effects in the region. The site effect plays a crucial role in planning and developing earthquake-resistant constructions as well as in estimating the damage caused by earthquakes. It is for this reason that the horizontal-to-vertical spectral ratio analysis has been used on ambient noise recorded in 13 sites in the region. Important site-specific parameters such as the fundamental frequency, f_0, of soft sediments and its corresponding amplification factor,A_0, alluvium thickness,H_0 and the soil vulnerability index,K_g, have been estimated for the sites. The fundamental site frequency for the study area ranged between 0.73 Hz to 11.00 Hz with their corresponding amplification factor also ranging from 1.6 to 10.0. The alluvium thickness ranged between 2.61 m to 175.75 m. The seismic vulnerability index which represents the likelihood of liquefaction ranged from 0.37 to 20.00. Tesano PS site appears to be the most vulnerable to earthquake destruction and liquefaction.

DEDICATION

I dedicate this work to my family, supervisors, and all staff and students of Kids at Heart International School.

ACKNOWLEDGEMENT

First and foremost, I thank the All-Powerful God for guiding me through this endeavour. All the praise belongs to him.

My profound gratitude goes to my supervisors, Dr. T. E. K. Armah and Dr E. A. Dzikunoo for their invaluable advice and support. I would also like to thank Prof. Ajei, Prof. Paulina Amponsah, Prof. Sakyi, Dr Ahulu, and Mr. Opoku for the pivotal roles played in this chapter of my life. I would also like to thank all the teaching and non-teaching staff of the Earth Science department, University of Ghana, for their help and support. I say thank you and may God richly bless you.

I express my gratitude to all of my friends and coworkers for their advice and encouragement.

TABLE OF CONTENT

LIST OF FIGURES

LIST OF TABLES

CHAPTER ONE

INTRODUCTION

1.1 Background

Earthquake intensity and damage do not solely depend on the magnitude and distance from the epicentre. They partly depend on the soil characteristics, the underlying geological conditions, and engineering structural integrity (Akkaya & Özvan, 2019; Cadet et al., 2011; Janusz et al., 2022; Mundepi et al., 2015; Tanjung et al., 2021). The soil's structure plays a significant role in increasing the region's earthquake risk as well as the severity of the earthquake damage. Adjacent regions subjected to the same seismic activity may experience damages of varying scale including ones at a distance or remote from the epicentre (Akkaya & Özvan, 2019; Bonnefoy-Claudet et al., 2009; Talha Qadri et al., 2015). In 2001, Ahmedabad (India) was severely affected by the Bhuj earthquake even though the city was 400 km away from the epicentre. This occurrence is due to the geology and younger alluvial deposits (Ranjan, 2005). Interestingly, soils that show stability under static stress may behave differently under dynamic stresses such as earthquakes causing failure and massive destruction to structures (Akkaya & Özvan, 2019). Thick soft sediments with less compaction generally amplify the earthquake waves the most (Bard, 1994; Bonnefoy-Claudet et al., 2006a; Tanjung et al., 2021). Comparatively, hard rock conditions cause the area experiencing an earthquake to record less damage (Damayanti & Sismanto, 2021). Vella et al. (2013) concluded that the thick layers of Oligocene-Miocene clay and marl greatly influence the site response of the Maltese island and have a strong link with some of the most damaging earthquakes recorded in the area. Gurler et al. (2000) emphasized the relation between the geology of Mexico and the damage recorded and observed during the 1957 and 1985 earthquakes in the country. Most of the damaged buildings were sited on soft clays which amplified the ground motion. Site effects refer to the variations in ground motion and seismic intensity felt at various regions as a result of the site's

geology and geotechnical characteristics. Site effects significantly impact the severity of earthquake damage. Notable examples of site effects include the Great Hanshin-Awaji earthquake in Kobe in 1995, where a magnitude of 6.9 with an intensity ranging between XI to XII on the Modified Mercalli Intensity Scale was observed (Bonnefoy-Claudet et al., 2009).

Site effects estimation has emerged as a key issue to address to mitigate and possibly prevent structural damage resulting from seismic ground motion (Cadet et al., 2011). Such estimations are critical because different sites exhibit particular seismic responses at which ground motion is amplified and has proved to be disastrous when it coincides with the fundamental frequencies of structures (Talha Qadri et al., 2015). Active fault zones and ground deformations also increase the risk of seismic hazards damaging infrastructure (Bray, 2009; Meghraoui et al., 2016; Murbach et al., 1999; Oettle & Bray, 2013). Bray (2009) highlighted that the performance of structures is greatly affected by site-specific factors such as fault characteristics, underlying surface geology, and the foundation of the structural system. Anastasopoulos et al. (2007) explained how the Atatürk Basketball Court in Turkey having its foundation overlying a displacement fault was significantly damaged beyond repairs. However, Murbach et al. (1999) showed that proper planning achieved less damage to some structures during the M 7.3 1992 Landers Earthquake event. In recent times, planning and management of urban areas have generally been based on economic considerations rather than geotechnical. These omissions during urban centre planning may result in greater damage than necessary with far-reaching economic and social implications in the event of a natural disaster (Chen et al., 2021; Janusz et al., 2022; Moustafa et al., 2022). For earthquakes, magnitudes, timing, and location cannot be predicted precisely. Hence, countries in both high and low-seismically hazardous areas have therefore invested in pre-disaster mitigation strategies like building codes that inform design criteria for new construction works and also reinforce old buildings as well as public awareness programs. These strategies show how prepared the areas are and in effect

can reduce damage to properties and loss of lives. These strategies involve estimating the seismic vulnerability of a particular area by evaluating site effect parameters such as the fundamental frequency and the amplification factor to aid in geotechnical planning of new structures and also guide re-enforcement or enhancement of old buildings (Bard, 1994; Bonnefoy-Claudet et al., 2006b). Seismic vulnerability maps have been developed through geotechnical investigations to assist engineers in determining where various structures can be sited based on the building codes.

Over the years, various categories of methods have sought to estimate the magnitude of amplification caused by soft sediments. Amplification of ground motion is a result of the impedance contrast existing between the bedrock and soft sediments deposited on them (Castellaro & Mulargia, 2009; Hunter et al., 2002; Nortey et al., 2018). Numerous instances of catastrophic earthquake effects in literature have shown the need to incorporate reliable analysis methods and procedures in site effect estimations (Marcellini, 2006). Methods that involve direct monitoring of ground motion through earthquakes are most effective and are limited to regions with high seismic activity rates. Such methods are less effective and rarely used in low to moderate seismic zones as it takes several years to collect enough reliable datasets. Recent site effect assessments in urban and densely populated areas are based on ambient noise (Bonnefoy-Claudet et al., 2006a; Janusz et al., 2022; Johnson & Lane, 2016; Liu et al., 2014). Ambient noise is a low-amplitude and short-period vibration sourced from natural disturbances such as wind interacting with structures and vegetation or from cars, heavy machinery traffic, and other sources (Bonnefoy-Claudet et al., 2009; De Guevara et al., 2022; Talha Qadri et al., 2015). Special physical parameters such as the fundamental site frequency, amplification factor, sedimentary thickness, and vulnerability index vary from place to place due to variations in local geology; hence, estimating these parameters from the ambient noise recordings aids in site response analysis. These site-specific parameters give engineers and

geoscientists an idea of just how much the soil can trap and amplify the seismic wave during an actual seismic event. One of the most effective methods used to achieve this is the horizontal-to-vertical spectral ratio (HVSR) analysis of ambient noise (Bonnefoy-Claudet et al., 2009; Mundepi et al., 2015; Nakamura et al., 2000).

The horizontal-to-vertical spectral ratio (HVSR), was initially presented by Nogoshi and Igarashi, but later developed by Nakamura and has proven to be an easy and reliable way of estimating local side effects over the years (Akkaya & Özvan, 2019; Bonnefoy-Claudet et al., 2009; Molnar et al., 2007b; Talha Qadri et al., 2015). The technique has been reviewed in depth by the SESAME (Site Effect Assessment Using Ambient Excitation) project (Marcellini, 2006). The project proposed a comprehensive list of guidelines for effective measures to take when using the method and has since been applied in several densely populated and low-to-moderate seismic areas for earthquake engineering purposes (Onyebueke et al., 2017; Vella et al., 2013). The technique is an experimental procedure used to evaluate some characteristics of soft sediments like the fundamental site frequency and amplification factor which are mostly adopted in micro zonation investigations. Just like any other geophysical method, the HVSR technique is not absolute and should be used together with other methods to fully characterize the complexities of soft sediments (Marcellini, 2006). Particularly, the HVSR technique underestimates the amplification factor to an extent but gives a reliable estimate of the fundamental site frequency (Field & Jacob, 1993; Parolai, 2012). Sediment thickness can be calculated from ambient noise using the HVSR technique. Sediment thickness is an equally important parameter in earthquake engineering and construction work as it plays a crucial role in the stability of building foundations (Bard, 1998; Field & Jacob, 1993; Tian et al., 2019). The soil vulnerability index can also be estimated using ambient noise measurements (Nakamura, 1997). A seismic soil vulnerability index assesses and quantifies the vulnerability of regions or buildings to earthquake hazards. The spectral ratios of ambient noise

simultaneously measured on structures and their foundation ground surface can be used to assess the seismic response characteristics of buildings (Nakamura, 1997). Numerous research has shown that this simple and cheap approach based on the HVSR analysis of ambient noise shows a good correlation with strong motion analysis such as earthquakes (Ullah & Prado, 2017). All these parameters are valuable tools for urban planning, risk reduction, and preparing for disasters in seismically active places. It helps authorities prioritize resources, implement building codes and construction standards, and plan emergency response strategies.

Active artificial seismic sources such as explosions or heavy mass drops are not appropriate in heavily populated regions for strong ground motion analysis (Chen et al., 2009). In the case of the Greater Accra Metropolitan Area (GAMA), the HVSR on ambient noise approach seems to be the most suitable method for site effect estimation because strong earthquakes very rarely occur and also there are few permanent seismographs installed for adequate ground motion monitoring (Amponsah et al., 2009). Even though the public's general perception is that seismic risk is negligible, historic records and recent tremors only indicate that the area is still seismically active and requires the needed attention. The recent increasing rate of urbanization in the GAMA due to the centralization of countless industries within it has caused a dramatic increase in building density since the last destructive earthquake. Buildings in the area are generally not constructed to be resilient and to withstand earthquake shocks (Ayetey & Andoh, 1988). Most of them have been mounted on a new diversity of geological conditions of which site effect conditions may not be known.

It is a crucial task for urban regions, as in the case of the GAMA, to have a concrete and appropriate plan of seismic hazard mitigation because it is at a high risk of earthquake destruction even though it is in a relatively low-to-moderate risk zone (Irinyemi et al., 2022; Kadiri & Amponsah, 2021; Meghraoui et al., 2019). Infrastructure engineers, town planners, and emergency response units including the National Disaster Management Organization

(NADMO) are constantly seeking high-resolution and accurate geotechnical information on assessing seismic damage, designing infrastructure to withstand earthquakes, and planning for and responding to emergencies. This research arises out of the need to improve and add to scientific and geotechnical knowledge concerning seismic risk to buildings in the GAMA and estimate potential risk zones for future buildings in the area using the horizontal-to-vertical spectral ratio approach.

1.2 Problem Statement

Evolving urban centres are strategically placed or located along river valleys, and alluvial fans besides mountains, coastal plains, and others because of the sufficient water supply that the thick aquifers located in such places may offer. The thick sediments harbouring these aquifers are good news for accessing water in urban centres but also increase the risk of potential high damage during earthquakes. Also, heavy weathering in such places results in the deposition of soft unconsolidated sediments often characterized by heterogeneous geological features. Such soils produce varying significant site effects (D'Amico et al., 2008). It has been established from numerous earthquake studies that the intensity and damage caused by strong ground motion are more often than not linked to such soft sediments (Chen et al., 2009; Chen et al., 2021). Figure 1 shows the cities of Accra and Tema, both urban centres in Ghana are located in the Main Volta basin. In some locations of Accra, the weathered sandstones form aquifers about 60 m thick (Ayetey & Andoh, 1988).

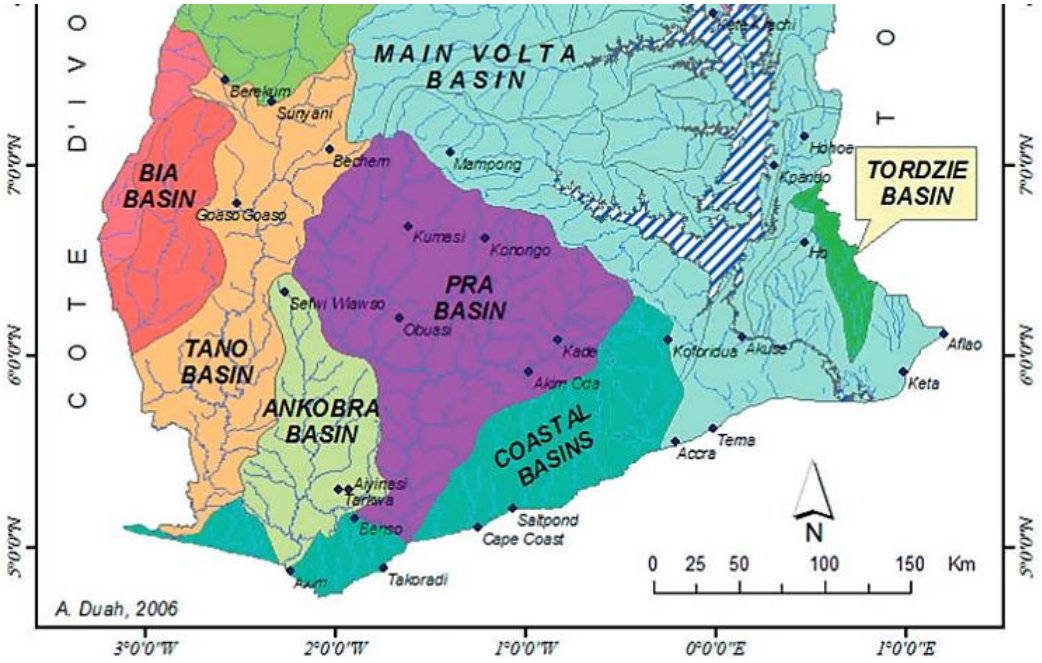

Figure 1 The main river basins in Southern Ghana (Gyau-Boakye et al., 2008)

Seismicity in Ghana is higher in the southern parts of the country due to the existence of active faulting of the two major faults; the Coastal boundary fault and Akwapim fault zone (Ahulu et al., 2018; Amponsah et al., 2009; Meghraoui et al., 2019). Most earthquakes in Ghana have had epicentres around the intersection of these two faults (Amponsah, 2004). The GAMA is located in a seismic zone with isoseismal lines that range in magnitude from seven to nine on the Mercalli scale (Ayetey & Andoh, 1988). In recent years urbanization and population growth have been increasing at a concerning rate in these same areas of the country, particularly in the Greater Accra Metropolitan Area, GAMA (Stow et al., 2016). This has led to an increase in building and infrastructure development, most of which has been sited without much consideration of the developing areas' seismic response. It can be predicted that several construction projects have been sited in seismically active regions, placing these structures in danger of severe damage in the case of significant earthquakes (Ayetey & Andoh, 1988).

There is an increased risk of induced seismicity where human activities such as hydraulic fracturing, wastewater disposal, enhanced oil recovery, and mining activities among others,

add to the stress around active faults (Doglioni, 2018; Foulger et al., 2017; Grigoli et al., 2017; Rubinstein & Mahani, 2015). The resulting induced earthquakes do not differ entirely from naturally occurring earthquakes in terms of magnitude but rather in their timing (Doglioni, 2018; Nicol et al., 2011).

A greater portion of Ghana's ever-increasing population resides in bigger cities such as Accra, Kumasi, and Tamale among others. As these cities continue to become urbanized, their population also increases (Adedini, 2022; Devendran & Banon, 2022). According to Devendran & Banon (2022), the Greater Accra Metropolitan Area (GAMA) can be regarded as the biggest urban centre in Ghana and also a megacity within Africa. From 2000 to 2016 the estimated population growth rate was 2%, this was projected to reach about 2.4% between 2016 and 2030 (Imoro Musah et al., 2020). Aside from this, there has been a general projection of a total population increase on the continent from 1.5 billion to an estimated figure of around 2.5 billion by 2050 with a startling 55% of this living in urban areas (Komacek et al.,2017). These estimates are bound to increase alarmingly in coming years according to studies. This implies that there will be an even greater portion of the population occupying the seismically hazardous zones such as areas in and around Accra in years to come.

The intensity of earthquakes depends largely on their magnitudes but also significantly on the local site conditions of the subsurface (Bard, 1994; Gospe et al., 2020). Generally, the soil through which the energy moves has the potential to amplify it thereby causing severe damage (Hunter et al., 2002). A greater part of Accra is covered with shallow soft soils which amplify seismic waves significantly (Nortey et al., 2018). Another issue of concern is that the earthquakes occurring here in the country are categorized as shallow-focused. The magnitude 6.5 Accra earthquake in 1939 is believed to have had a depth of focus of 13.4 km (Kutu, 2013). Shallow-focused earthquakes with magnitude ranges of 4.0 to 6.0 pose a higher risk of destruction than deep-focused earthquakes, especially in heavily populated areas with few

earthquake-resistant buildings (Camelbeeck et al., 2022; Nappi et al., 2021). Induced seismicity further adds to this risk (Grigoli et al., 2017; Nievas et al., 2020).

1.3 Justification

In earthquake-prone areas, seismic hazards must be clearly defined to influence the design of earthquake-resistant structures fundamentally. The Ghana Standards Authority's Ghana Building Code (GhBC) GS 1207:2018 clearly states essential building requirements concerning earthquake hazards. Several methods such as deterministic seismic hazard analysis, probabilistic seismic hazard analysis, and the V_s^{30} has been used to understand and fully assist with construction work.

In most developing and even developed countries, pre-earthquake damage reduction strategies have proved costly when hazard models and maps underpredict or overpredict the hazard. The cost of re-enforcing old buildings and materials needed to build new resistant ones may be too much to bear. In places like Ghana where previous hazard models and maps were based on assumptions and preconceptions of researchers, there is a possibility of inaccurate hazard estimates. It has, therefore, become imperative to consider how a hazard model and a hazard map predict and how to significantly enhance their estimations.

The horizontal-to-vertical spectral analysis of ambient noise is a method that has proven to achieve a similar but convenient result. It provides a better understanding of the subsurface concerning how it may behave when seismic energy propagates through it and shows how much amplification the soil offers. In effect, it gives a clearer correlation between site response and the outcrop geology. This work seeks to provide supplementary knowledge that can inform site-specific parameters for construction work done in the high seismic vulnerability zones using the horizontal-to-vertical spectral analysis.

1.4 Objectives

The main aim of this study is to come up with a seismic vulnerability index map and site-specific parameters that can supplement existing literature.

To achieve the main objective, the specific objectives are:

- To determine the fundamental frequency of selected sites and its corresponding amplitude
- To calculate the seismic vulnerability index for these sites
- To estimate the thickness of the sedimentary cover
- To categorize the selected sites into seismic vulnerability zones by using the obtained parameters to generate a vulnerability map in ArcMap.

1.5 Study Area

The Greater Accra Metropolitan Area (GAMA) covers the majority of the Greater Accra region in Ghana, encompassing Accra Metropolis, Ashaiman, Tema Metropolis, Ga East, Ga South, Ga West, Adenta, and Ledzokuku Krowor as shown in Figure 2 (Nortey et al, 2018; Owusu, 2012). The size of the GAMA is approximately 1550.37 km^2 land area and is bounded between latitudes 5º45'0''N and 5º25'0''N and longitudes 0º30'0''W and 0º05'0''E along the Atlantic coast of Ghana.

The area is mainly undulating in the east grading into the Accra plains. There are recognizable high ranges such as the Akwapim ranges trending from northeast to southwest (Ayetey & Andoh, 1988). There are a few isolated hills and rock outcrops scattered across the region, which range from flat to gently undulating slopes rising to 75 meters at the foothills (Addae & Oppelt, 2019).

The GAMA has experienced a constantly increasing rate of urbanization over the past years from a group of fishing communities and has developed into Ghana's economic centre,

attracting investors from all over the country and the world. The GAMA is currently the most economically industrialized region in Ghana (Allotey et al., 2006). According to the report by Addae & Oppelt (2019); Nortey et al. (2018); and Imoro Musah et al. (2020), it has a population that approximates to about five million and is expected to double in 20 years making it the largest metropolitan by population.

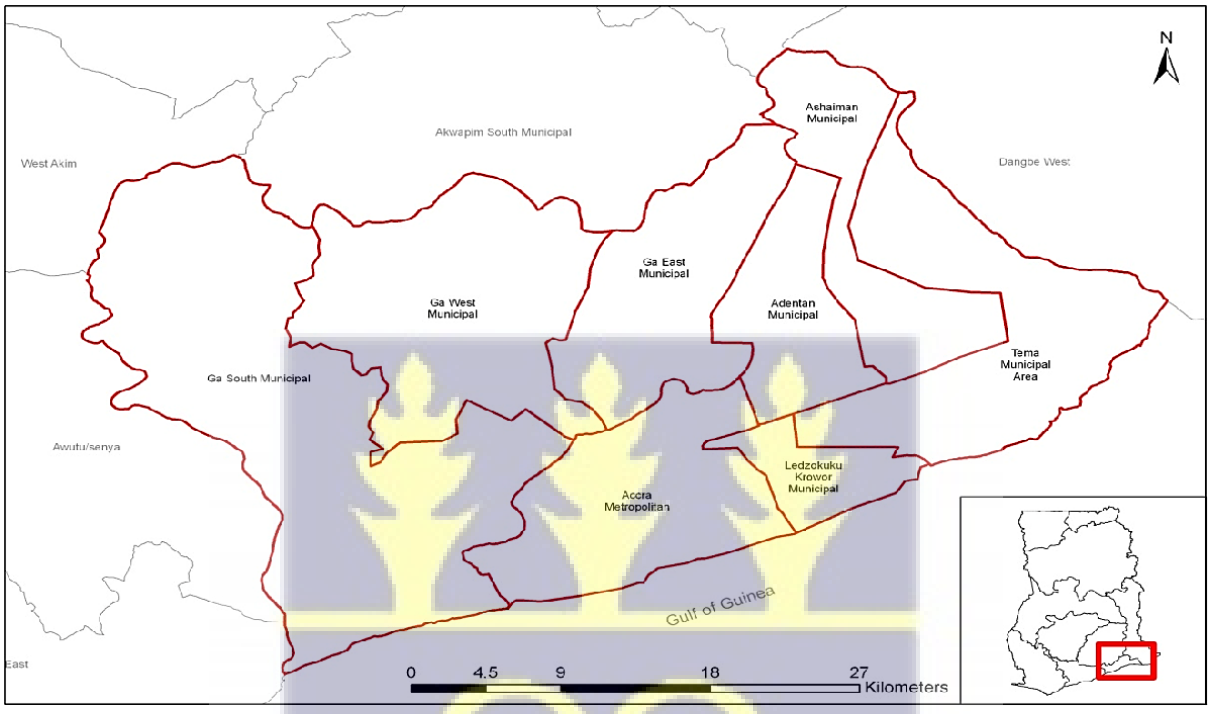

Figure 2 Map of the Greater Accra Metropolitan Area (GAMA) (Owusu, 2012)

1.5.1 Geological Setting

The geological makeup of the GAMA as indicated in Figure 3, is fairly simple. According to Ayetey & Andoh (1988), the basement rocks to the east of the Akwapim hills are generally of the Dahomeyan series; metamorphosed Precambrian sediments which are predominantly hard, foliated, and folded gneisses. The Dahomeyan series are overlayed with the much younger Togo series rocks which are hard quartzites or recrystallized sandstones. The Togo series is characterized by interbedded quartz and mica schist which are folded, faulted, and mainly trend northeast to southwest. Rocks of the Accraian formation underlie most of the central part of

the study area. The Accraian formation consists of mainly Devonian shales and interbedded sandstones.

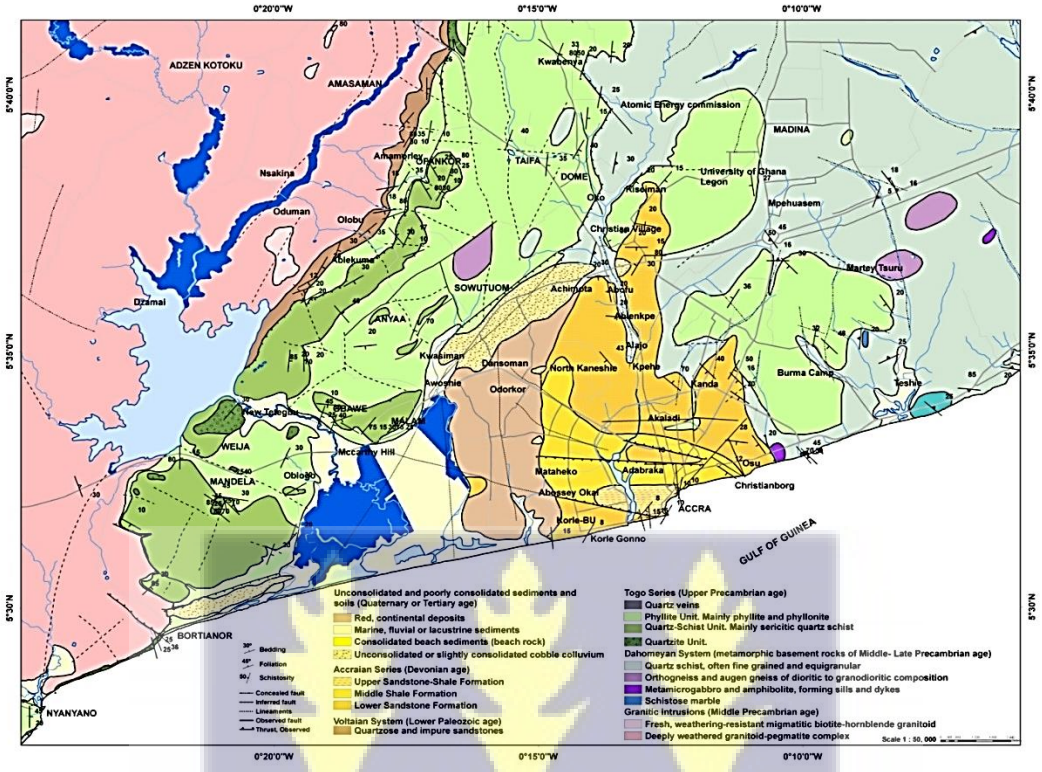

Figure 3 Geological Map of the GAMA (Dawood et al., 2012)

1.5.2 Engineering soil distribution concerning bedrock topography

Residual soils form a complex spatial distribution and the process is generally controlled by bedrock, drainage, and topography. These soils are made of patches of lateritic soils on higher ground and sands and clays on lower ground, primarily depending on whether the bedrock is made up of sandstones, quartzites, or shales (Ayetey & Andoh, 1988; Nortey et al., 2018). Figure 4 represents a map developed using data from Accra boreholes that were drilled for site investigations (Ayetey & Andoh, 1988).

In low-lying areas, the Accraian interbedded sandstone and shale deposit typically produce fine to coarse sands, which become silty to clayey where shales are interbedded. However, on higher terrains with satisfactory drainage, lateritic soils that range from sandy to gravelly are

more dominant. The shale series normally forms the clays. In low-lying places, the Togo series often produces fine to coarse sand that ranges from gravelly laterites to highly quarzitic cobbly to gravelly laterites on high ground, with the schist zones producing clayey to silty sands. The Dahomeyan rocks undergo weathering to form residual soils with thick clay and silty-sandy clay in river channels and valleys. Generally, alluvial deposits are of clayey to silty material (Ayetey & Andoh, 1988; Junner, 1941). The depth and products of weathering of these formations can be used to determine seismic risk in these areas (Amponsah et al., 2009; Amponsah et al., 2008). These soft residual soils may amplify seismic energy rendering such areas highly vulnerable and at risk of earthquake damage.

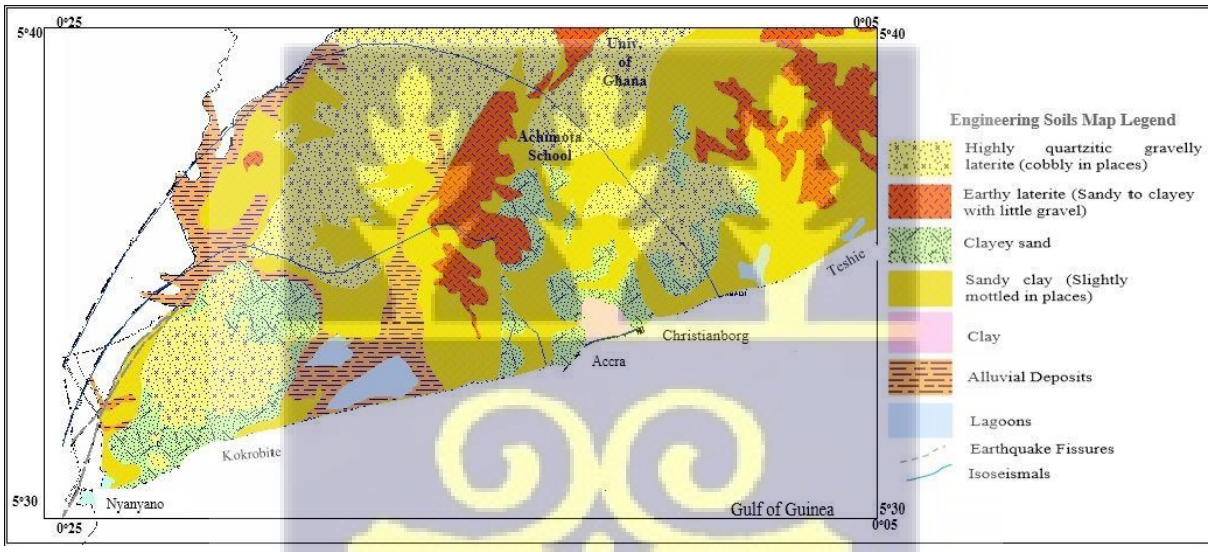

Figure 4 Engineering soil map of the Accra area with isoseismal of the 1939 Earthquake (Nortey et al., 2018)

1.5.3 Seismotectonic of the GAMA

Southern Ghana is known for being the most seismically active part of the country. Three separate tectonic zones, with varying tectonic features, make up the seismotectonic of Southern Ghana as well as its off-shore area. These tectonic zones are the Akwapim fault zones, the Romanche fracture zone, and faults in the shelf and coast mainly comprised of the Coastal Boundary fault. The majority of recent earthquakes and tremors have occurred along the Akwapim fault zones and the Coastal boundary fault (Ahulu et al., 2018).

1.5.3a Akwapim Fault Zones

This is a system of thrust faults trending from southwest to northeastwards through Kpong, Ho, and into Togo and Benin. The fault zone is outlined by the Western Boundary Fault (WBF) and the Eastern Boundary Fault as shown in Figure 5. In recent years, the zone has undergone a block-tectonic style of deformation that has resulted in several normal faults developing (Ahulu et al., 2018; Amponsah et al., 2012). Some faults in this zone include the Akwapim fault and the Nyanyanu fault.

1.5.3b Faults in the coastal area and shelf

The 1939 earthquake sparked a series of research into understanding the seismotectonic of Southern Ghana. Analysis of knowledge on land geology and interpretation of seismic reflection survey of the continental shelf led to the discovery of the presence of some faults in the area as per Blundell (1976). The Coastal Boundary Fault is the most prominent normal fault in the shelf (Amponsah et al., 2012). It trends east-west as shown in Figure 5. It intersects the Akwapim fault just to the west of Accra. Blundell (1976) explained that the Coastal Boundary Fault forms the northern margin of the Keta Basin. Other faults in this zone that are believed to be active include the Fenyi-Yakoe and Adina faults (Amponsah et al., 2012)

1.5.3c Romanche Fracture Zone

Figure 5 shows the Romache Fracture Zone (RFZ), an offshore fault system that runs almost parallel to the coastline. It is an inactive transform fault of the Mid-Atlantic Ridge which differentiates the continental crust from the oceanic crust (Attoh et al.,2005).

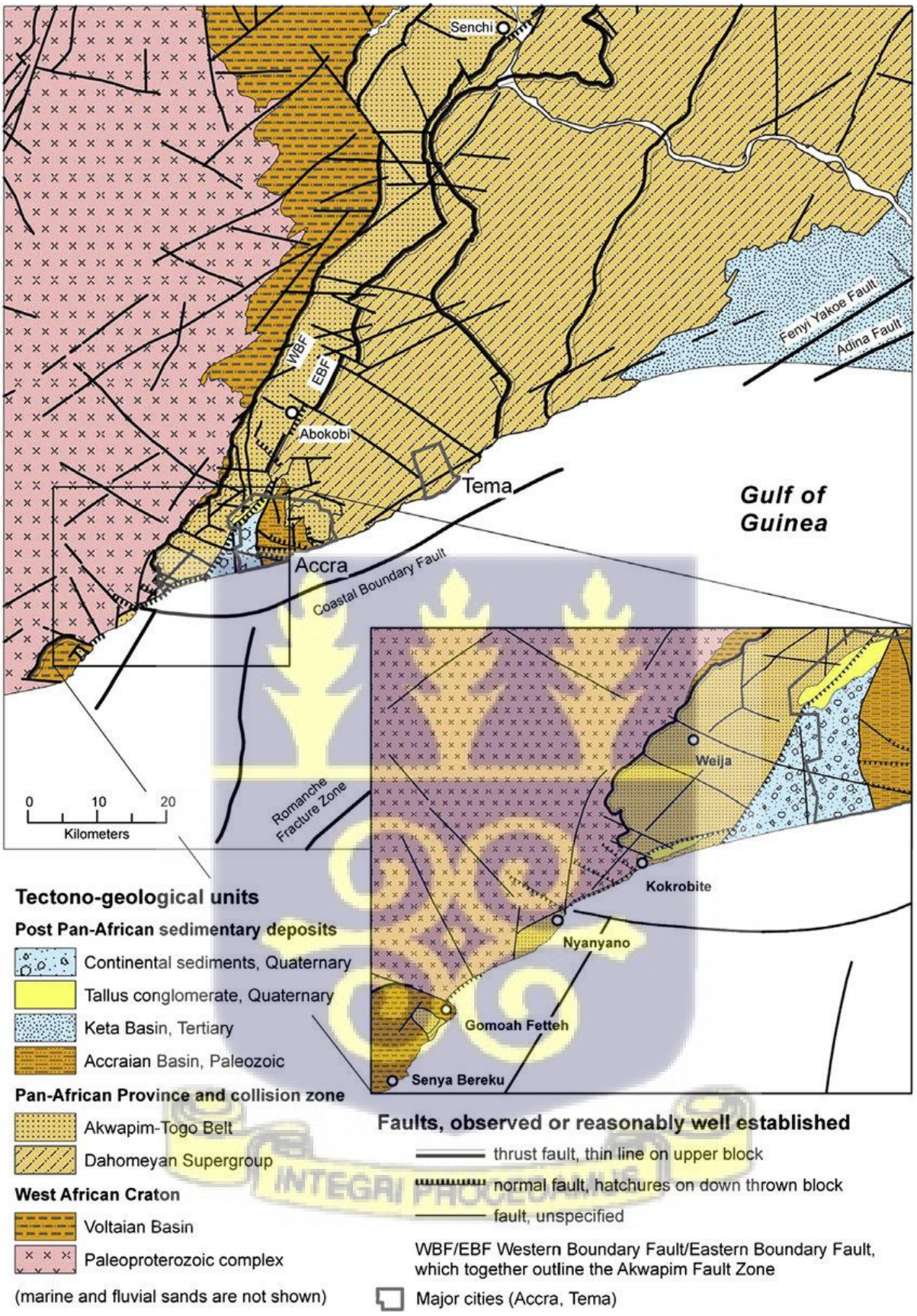

Figure 5 Neotectonics and Geological sketch map of South-East Ghana (Amponsah et al., 2012)

1.5.4 Neotectonics of Southern Ghana

A study by Amponsah et al., (2012) on the tectonic-structural evolution of Southeast Ghana, made clear the fact that the forces that caused deformation during the Pan-African orogenesis no longer exist in the present day. However, discoveries of high-to-moderate- angle neo-tectonic normal faults indicate that tectonic movement is still ongoing (Amponsah et al., 2012). Such faults are believed to be utilizing weakened zones and hence may mimic the older Pan-African fault directions. Neo-tectonic faulting is believed to be greatly involved in modern-day seismic activity in the area. The study predicts that there could be more such faults existing than known either from topographic analysis or interpretation of drill holes in the Akwapim Togo belt. The reason is that there is usually an absence of contrasting lithologies and also thick soil cover keeps them hidden.

Ghana's continental margin subsides, exerting a shearing force that is believed to be the resulting factor of the occurrence of the numerous neo-tectonic normal faults in the coastal area and shelf. Lithological heterogeneities in the crust and pre-existing structures are also contributing factors to the formation of such normal faults (Amponsah et al., 2012). Such faults can be located in areas such as Abokobi, Nyanyano-Kokrobite, and to the West of Accra, the southernmost section of the EBF as shown in Figure 5.

CHAPTER TWO

LITERATURE REVIEW

2.1 Seismicity of Africa and Ghana

The African plate has had its share of destructive earthquakes as have the other plates in other major earthquake zones. In major earthquake zones, such as Chile, the subduction between the Nazca plate and the South American plate causes very large earthquakes (Leyton et al., 2009). These earthquakes are referred to as inter-plate earthquakes and usually have comparatively high magnitudes. Africa experiences intraplate earthquakes which are generally considered to be a result of the presence of some major active faults in the continent (Meghraoui et al., 2016). Figure 6 shows the earthquake zones within the African plate.

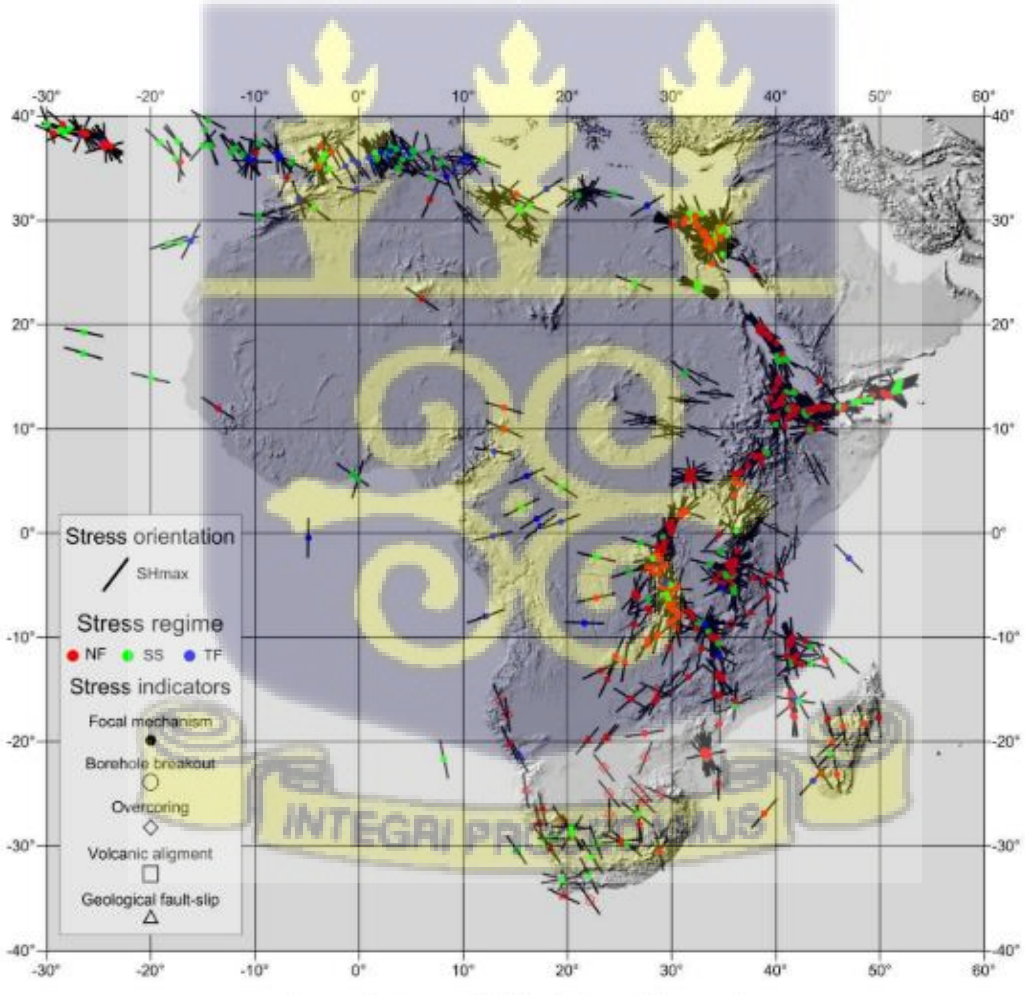

Figure 6 Stress Fields within the African Plate. Earthquakes within the plate is centred around these faults(Craig et al., 2011; Fairhead & Girdler, 1971; Meghraoui et al., 2016)

Notable cases of earthquakes in recent years include the magnitude 6.2 Karonga earthquake in Malawi in 2009, the magnitude 6.0 Bukavu earthquake in the Democratic Republic of Congo in 2008, the magnitude 6.8 Zemmouri-Boumerdes earthquake in Algeria and the magnitude 7.1 Juba earthquake in South Sudan (Meghraoui et al., 2016) Areas around the East African Rift System and North Africa thrust and fold belt such as the Maghreb in Northern Africa are classified as high seismic zones (Kadiri & Kijko, 2021). West Africa is generally considered to be a zone of low-to-moderate seismicity with occasionally large-magnitude earthquakes even though it is considered remote and a huge distance away from major active plate boundaries as shown in Figure 7 (Amponsah et al., 2009; Amponsah et al., 2012; Attoh et al., 2005; Campbell et al., 2018; Kadiri & Kijko, 2021). Additionally, the Southern African plateau is also known to be seismically active (Meghraoui et al., 2016).

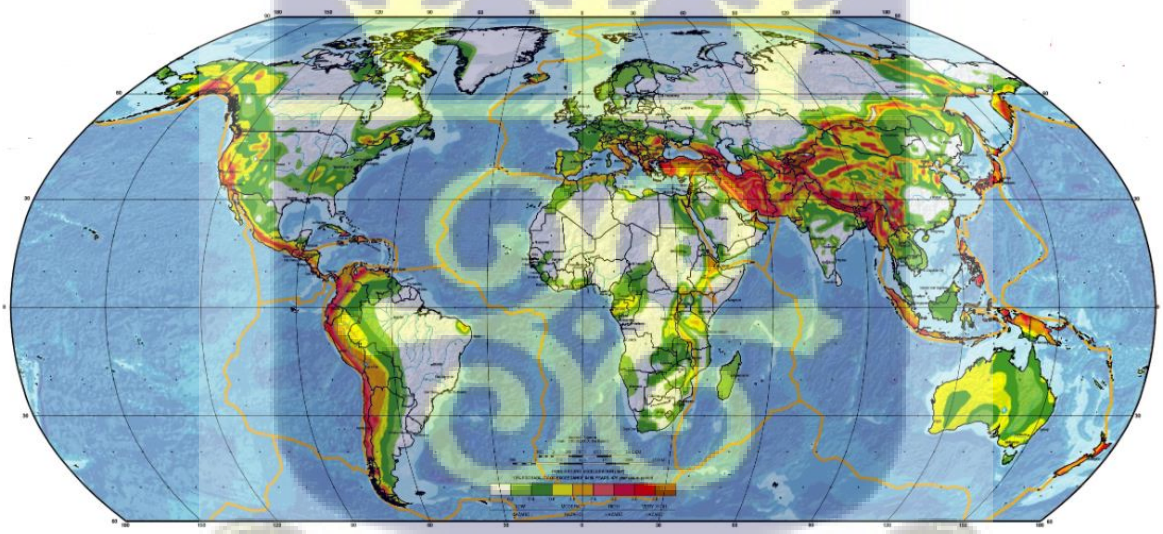

Figure 7 A Global Seismic Hazard Map depicting areas of a probable high level of ground shaking during earthquakes. Africa experiences relatively moderate ground-shaking (Giardini et al., 1999).

The mention of earthquakes in Ghana does not strike as much fear and panic as it would in different parts of the world. This is because of the seeming distance of our location from the

major earthquake zones leading many to believe that largely destructive earthquakes are not likely to occur in the country.

The southern part of Ghana has experienced countless earthquakes even before proper recording instruments were introduced. Few of these have been destructive and led to the loss of lives and property dating as far back as 1615 (Amponsah, 2002; Amponsah et al., 2009, 2008; Meghraoui et al., 2019; Nortey et al., 2018; Osei et al., 2018). Notable ones among these include the 22nd June 1939 earthquake (Mw=6.5 on the Ritcher scale) with an intensity of IX on the Modified Mercalli scale and the 1862 earthquake (Mw=6.5 on the Ritcher scale) with an intensity of IX on the Medevedev-Sponheuer-Karnik scale(Amponsah et al., 2008; Amponsah et al., 2020; Meghraoui et al., 2019; Quaah, 1982). It has been estimated that to add to the cost of damage to infrastructure, the 1939 earthquake killed seventeen people and injured a number close to 135. The major shocks in 1862 left the Christiansborg Castle and several forts uninhabitable (Junner, 1941). A magnitude 5.7 with intensity IX in 1636 caused a gold mine to collapse in the Axim district (Nortey et al., 2018). Ahulu et al. (2018); Amponsah et al. (2009); Osei et al. (2018); and Nortey et al. (2018) are just a few of the numerous studies that have been conducted to clearly understand the sources of these earthquakes that occur in southern Ghana to help improve seismic hazard assessment in the area. The seismic activities in Ghana are believed to be a result of possible movement along various thrust faults including the Togo, Birimian, and Dahomeyan (Amponsah et al., 2020; Bondesen & Smit, 1972). These pre-existing zones of weakness when reactivated become sources of intraplate earthquakes (Al-Halboosi et al., 2022; Leite Neto et al., 2022; Sykes, 1978).

Earthquakes do not necessarily kill, but rather poor structures sited upon the ground where the energy passes are the cause of most earthquake-related fatalities. Earthquake engineering analysis is mainly geared towards predicting the response of structures to particular levels of ground shaking and this is the closest we can get in trying to reduce the damage it causes.

Several approaches have been developed and new ones are constantly being sought after to maximize the knowledge about estimating the possible damage that can result from an earthquake on a site. Some of these are based on data on ground shaking intensities during past earthquakes.

2.1 Probabilistic Seismic Hazard Analysis.

The probabilistic approach considers a catalogue of earthquakes that have occurred at a particular site and uses this data to analyze and predict ground shaking intensity and magnitude of a future earthquake. A source zone, possibly a fault, needs to be identified. The source zone is expected to host a future earthquake. Areas surrounding the source zone are demarcated into sections based on how much ground shaking intensity can be produced some distance away using a predicted magnitude. The accuracy of this approach greatly depends on the earthquake catalogue and the source zone among others. Aside from the seismic source zone, the effectiveness of the method also depends on the equations for predicting ground motion and the seismic source parameters. The final product of this approach is a seismic source model which can be used to predict what the seismicity of the source zone will look like over some time and also the ground shaking intensity at a specific area close to the source (Baker et al., 2013). Earthquake engineers use this analysis to help construct more resilient structures in earthquake zones. The Probabilistic Seismic Hazard Analysis approach has been employed in Ghana to produce a seismic hazard map for southern Ghana by Ahulu et al. 2018 and the seismic hazard map obtained after the study is shown in Figure 9 for a 10% probability of exceedance for peak ground acceleration of 50 years. Ahulu et al. (2018) concluded that out of the areas studied in southern Ghana, the Accra and Tema areas are found to be in the highest hazard zone in Ghana. Other significantly moderate hazard zones are found in places around Ho, Koforidua, and Akosombo. The paper admits to the difficulties faced in identifying seismically active fault zones in Ghana mainly because there are fewer than adequate stations

to properly monitor and fully understand the faults in terms of geometry, slip rate, and fault segmentation length among others. Nonetheless, three seismic source zones were identified in that study. They include the offshore zone in the Gulf of Guinea, the Accra zone, and the zone to the NNE of Ho (Figure 8). Seismic source parameters for each source zone were determined based on engineering seismology standard assumptions. Ground motion models that have been developed for areas in comparatively stable intra-plate regions with low seismic activity levels were selected for this study. The models used were derived using information from South Eastern Australia and Central and Eastern America since these areas bear a geographical resemblance to Ghana. The earthquake catalogue data used in this study initially contained a total of 127 events from different sources compiled between the periods of 1615 – 2009.

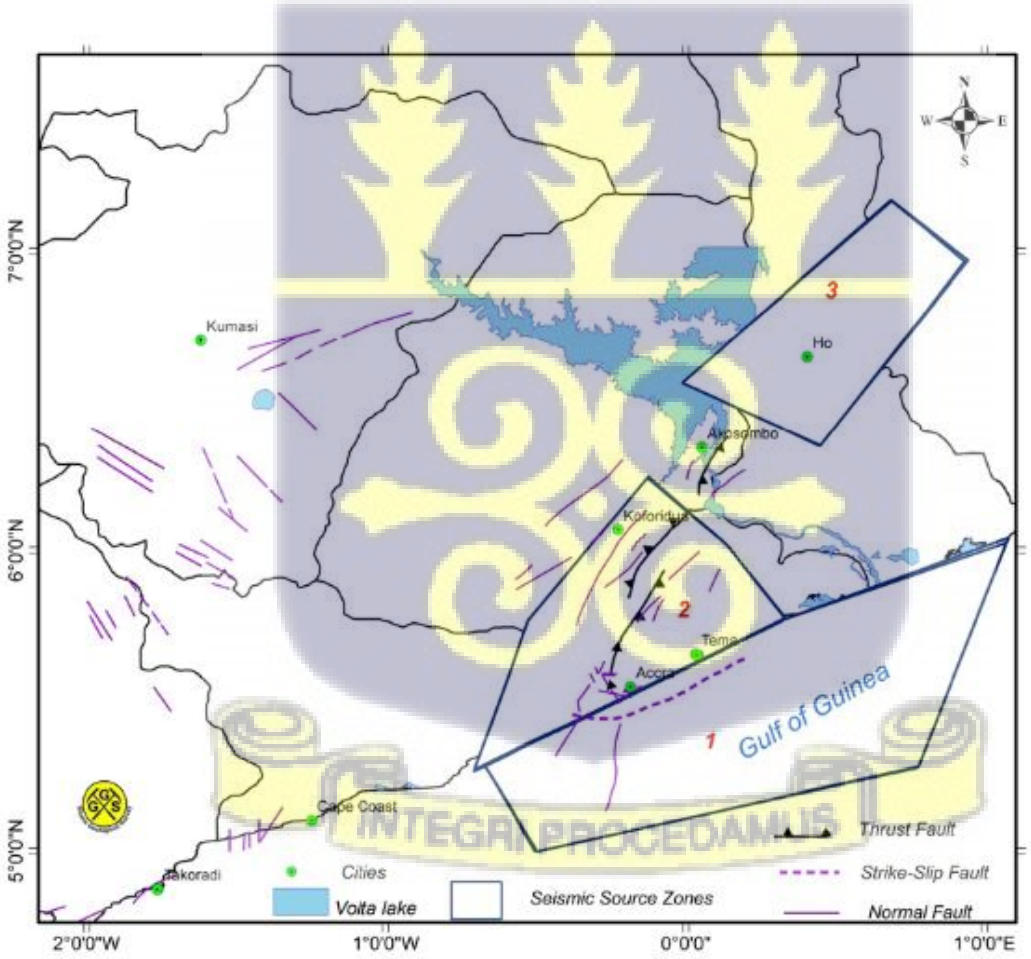

Figure 8 Seismic source zones used in the study (1 – offshore zone, 2 – Accra zone, 3 – NNE of Ho zone) (Ahulu et al., 2018)

After various analysis was run on the data, earthquakes with magnitudes $Mw < 4$ were excluded from the working catalogue mainly because most of them were foreshocks, aftershocks, and earthquake swarms whose magnitudes are considered too small to cause significant damage. A remainder of 33 events were used. The estimated peak ground acceleration for Tema and Accra was $0.20\ g$ and by the attenuation law, seismic hazard reduces as distance from the Accra/Tema region increases by a value of $0.05\ g$ for every $140\ km$.

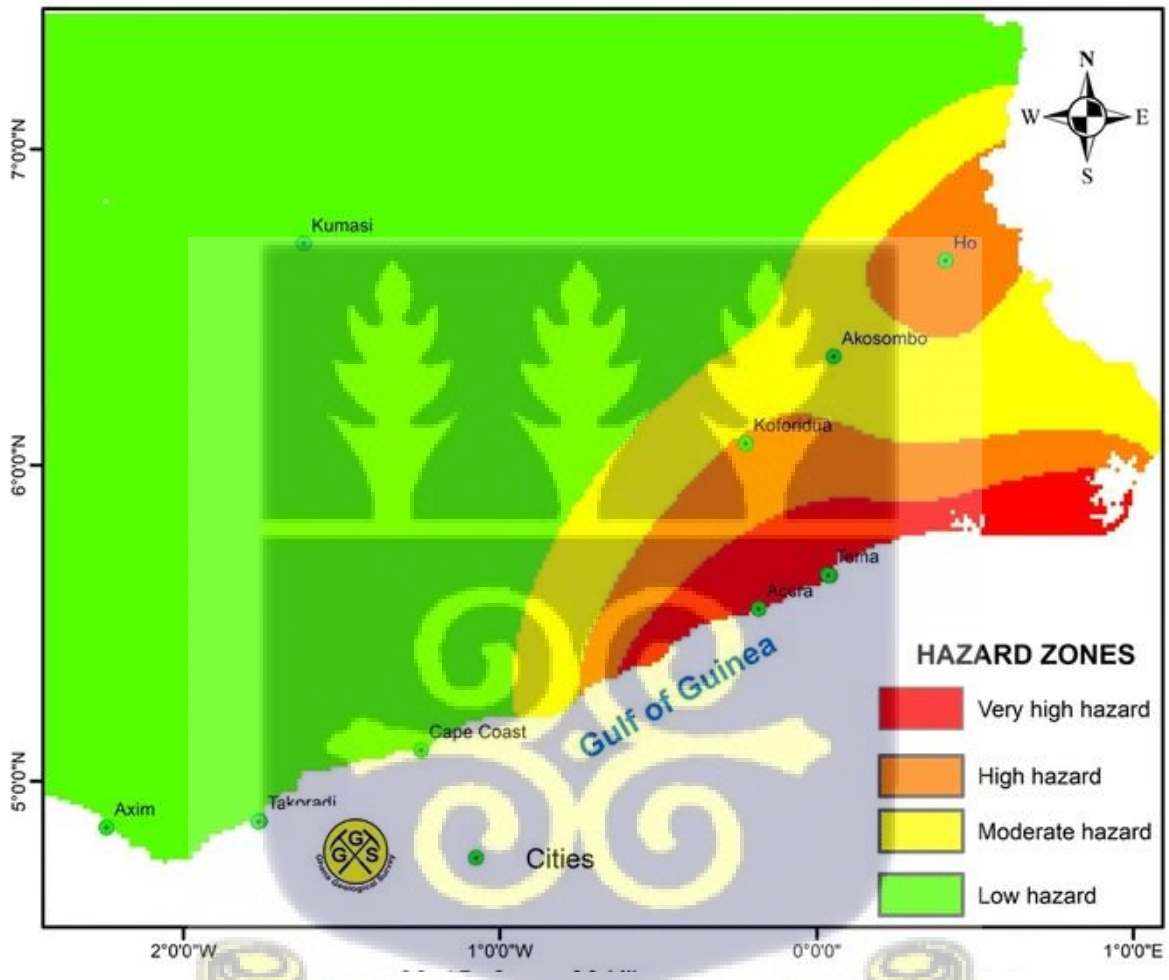

Figure 9 Seismic hazard map for southern Ghana as per the probabilistic approach (Ahulu et al., 2018).

The Probabilistic Seismic hazard approach which has also been used with an even broader catalogue for a period between 1615 – 2018 for earthquakes within West Africa estimated similar results for southern Ghana. The model predicted a worst-case scenario seismic event of magnitudes 5.5 – 6.0 (Irinyemi et al., 2022).

2.2 Monte Carlo-Based Seismic Hazard Model

The Monte Carlo approach is one of the many techniques in literature listed under the probabilistic approach to seismic hazard assessments. It is employed in areas considered to be stable continental regions such as Ghana with scanty seismological data and lower rates of seismic activities. Osei et al. (2018) hold the view that this method seems most desirable in the area because the conventional probabilistic method heavily relies on past seismic activities. The technique has been employed in six cities in the southern part of Ghana; namely, Accra, Tema, Ho, Cape Coast, Koforidua, and Akosombo to access seismic risk and ground motion intensities. The computations involved are straightforward and it also enables the analyst to identify the likely earthquake scenarios that can be chosen for further structural analysis. The only probable step-back of the method is the need for a significant number of simulations to arrive at a true solution since it is based on the use of random numbers (Osei et al., 2018). For this study, the research considered the earthquake catalogue compiled by Amponsah et al. (2012) from the period of 1615 – 2003 but excluded magnitudes less than 3.0 because they are generally regarded as not potent enough to cause damage. Two source zones were used in the model as opposed to the three used in the probabilistic approach used by Ahulu et al. 2018. Source zones for source characterizations are delineated considering historical and instrumental data recording in the zones, this research did not consider the third one because it contained too few a number to be considered variable (Figure 10). The Monte Carlo simulation algorithms were run to generate a synthetic earthquake catalogue with similar characteristics as the historically and instrumentally compiled ones. According to the researchers, ground motion prediction equations considered for the study are based on stable continental regions while the ones used by Ahulu et al. (2018) were for active-shallow-crust regions. These differences in procedure and assumptions led to a significant difference in the values obtained by both techniques (Table 1). The Monte Carlo approach obtained lower peak ground acceleration but both predicted higher seismic risk in both Accra and Tema. Tema however

shows a higher seismic hazard when compared to Accra. Ho and Cape Coast are at a relatively low seismic hazard.

Table 1 PGA estimated values based on the Probabilistic and Monte Carlo approach

City	Location		$10\ \%\ in\ 50\ years$	
	Longitude	Latitude	Probabilistic approach (Ahulu et al., 2018)	Monte Carlo Approach (Osei et al., 2018)
Accra	-0.182	5.555	0.2	0.05
Akosombo	0.050	6.346	0.06	0.06
Cape Coast	-1.255	5.100	0.026	0.01
Ho	0.408	6.649	0.1	0.02
Tema	0.035	5.657	0.2	0.04
Koforidua	-0.226	6.068	0.08	0.05

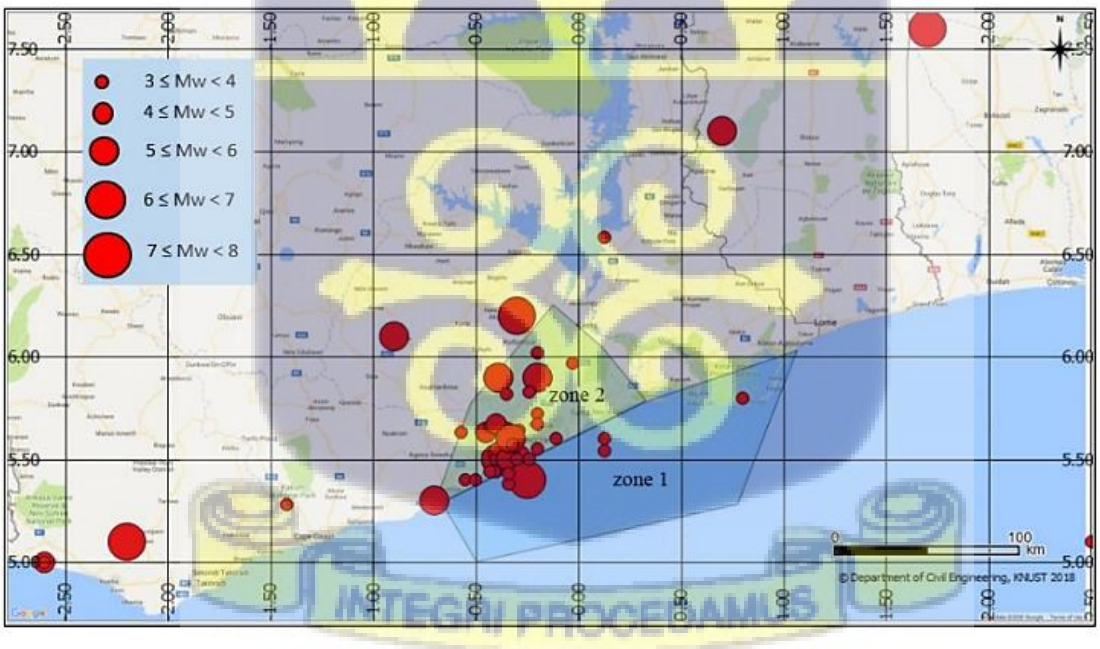

Figure 10 Seismic source zones in southern Ghana showing activities as complied in the 1615 – 2003 catalogue (Osei et al., 2018).

2.3 Deterministic Seismic Hazard Analysis

This analysis takes a slightly different approach when compared to the probabilistic analysis. The deterministic approach tries to predict the worst damage that can happen at a selected site when an earthquake of the highest possible magnitude happens. This method allows engineers to design buildings considering this worst-case scenario. This gives the deterministic approach an edge over the probabilistic because, for very important structures where a future earthquake failure would be unpardonable, the use of the deterministic approach is recommended since the analysis is made based on the worst-case scenario (Krinitzsky, 1995). The method is relatively simple to perform and involves less complicated calculations. However, it faces the same problem of inadequate knowledge of seismically active sources, as some faults remain hidden. A source zone is identified just as in the probabilistic approach. The second step is to calculate and model the largest expected earthquake that can occur in the source zone identified. Lastly, the ground motion analysis is done (Krinitzsky, 1995).

Amponsah et al. (2009) employed the deterministic method in some areas of Accra to evaluate ground motion intensity where a particular source zone and site conditions can control seismic hazards in the site. A bedrock model and a model for lateral changes in soil properties of subsurface rock were built for the analysis. The site conditions in the area studied are controlled mainly by the depth and the product of the weathering of bedrock. These are mainly from unconsolidated layers of soil which are known to amplify ground motion. Ground motion parameters are important in such modelling since they are site-specific and characteristic of these layers. Ideally, the ground motion parameters used for such analysis are determined from seismic refraction surveys, borehole investigations, and strong ground motion records. Strong ground motion data is not readily available in Ghana. The research, therefore, justified the use of synthetic data based on theoretical and computer simulations instead. Damages on buildings greatly depend on these ground motion characteristics. The research considered the magnitude

6.5 1939 with a maximum intensity of IX earthquake during the analysis to simulate the worst-case scenario. Computations of synthetic seismograms were generated using the models and the earthquake along the profiles A-A", B-B", C-C" and D-D" shown in Figure 11. The results obtained for the peak ground acceleration and peak ground velocity values range from $0.14\ g\ to\ 0.57\ g$ and $9.2 cms^{-1}$ to $37.1 cms^{-1}$ respectively. The peak ground acceleration values can produce an intensity of VII to IX on the Modified Mercalli Intensity (MMI) scale and IX to XI on the Mercalli-Cancani-Sieberg scale (MCS). The peak ground velocity can also produce an intensity of IX to XI on the MCS scale and VII to $VIII$ on the MMI scale. In conclusion, high-intensity levels of XI (MCS) and $VIII$ (MMI) have been estimated in the study area using the 1939 earthquake. This means should the Accra metropolis be hit by a similar or greater earthquake, there will be greater destruction and massive loss of human life. The largest shakings were recorded in places underlain by unconsolidated sediments with poor mechanical properties such as the ones found in the colluvium and continental and marine deposit areas in Figure 11.

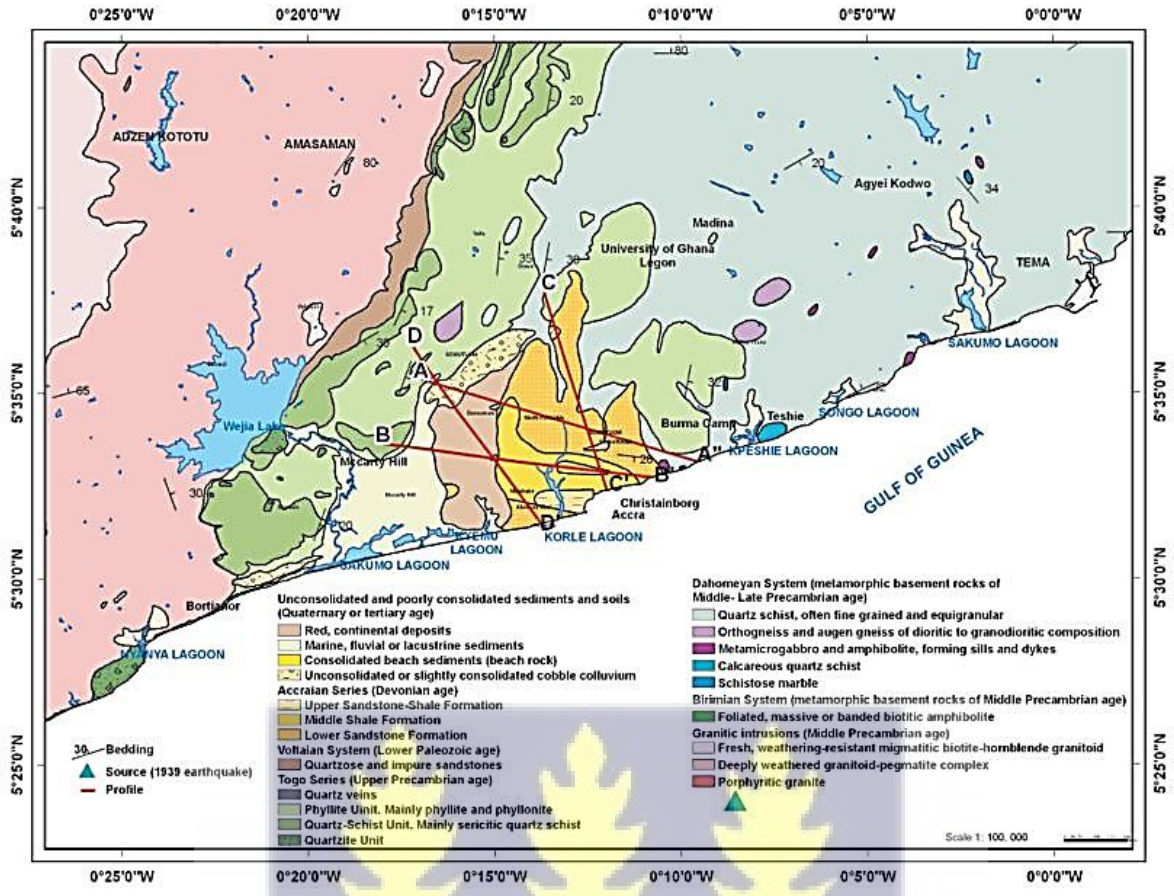

Figure 11 Geological map of southern Ghana showing the profiles used in the study (Amponsah et al., 2009)

2.4 V_s^{30} Mapping

Poor soil conditions amplify seismic waves to a great extent, adding to the damage that earthquakes pose. The velocity with which the shear wave travels through the soil carries a lot of information about the soil's behaviour and stiffness. The V_s^{30} mapping approach gives the average shear wave velocity in the top 30 m of soil and has thus, grown popularity in site characterization in seismic hazard analysis. The V_s^{30} values obtained using the Multichannel Analysis of Surface Waves (MASW) are used to create a soil classification map based on soil stiffness and response to seismic waves. The soil classification map created is critical for earthquake engineering purposes (Brown et al., 2000; Castellaro & Mulargia, 2009; Nortey et al., 2018; Rošer & Gosar, 2010). Nortey et al. (2018) studied the complex shallow soil distribution in Accra using the V_s^{30} and inferred results that are similar to previous site response

analyses in the area. The shear wave velocities obtained corresponded to soil profiles C and D, as per standards from the National Earthquake Hazards Reduction Program (NEHRP) classification scheme (Nortey et al., 2018). Soil profiles C and D represent shallow weathered rock ($> 6m \ < 30\,m$) and deep stiff soils ($> 30\,m$) respectively based on the shear wave velocity ranges obtained. The values are $360\ m/s \leq V_s^{30} \leq 760\ m/s$ for site class C and $180\ m/s \leq Vs30 \leq 360\ m/s$ for site class D which both show a significant difference in soil response to seismic energy. The southern part of Accra falls within site class D which shows low shear wave velocity as compared to the standards of the NEHRP and IBC indicating that it is vulnerable to high damage should there be an earthquake (Figure 12). Areas within site class C will better respond to earthquake shaking and might record less damage as compared to areas under site class D. It was difficult to establish a clear relationship between the velocity values obtained and the lithology of some other places of interest within the study area. Figure 12 shows the results obtained.

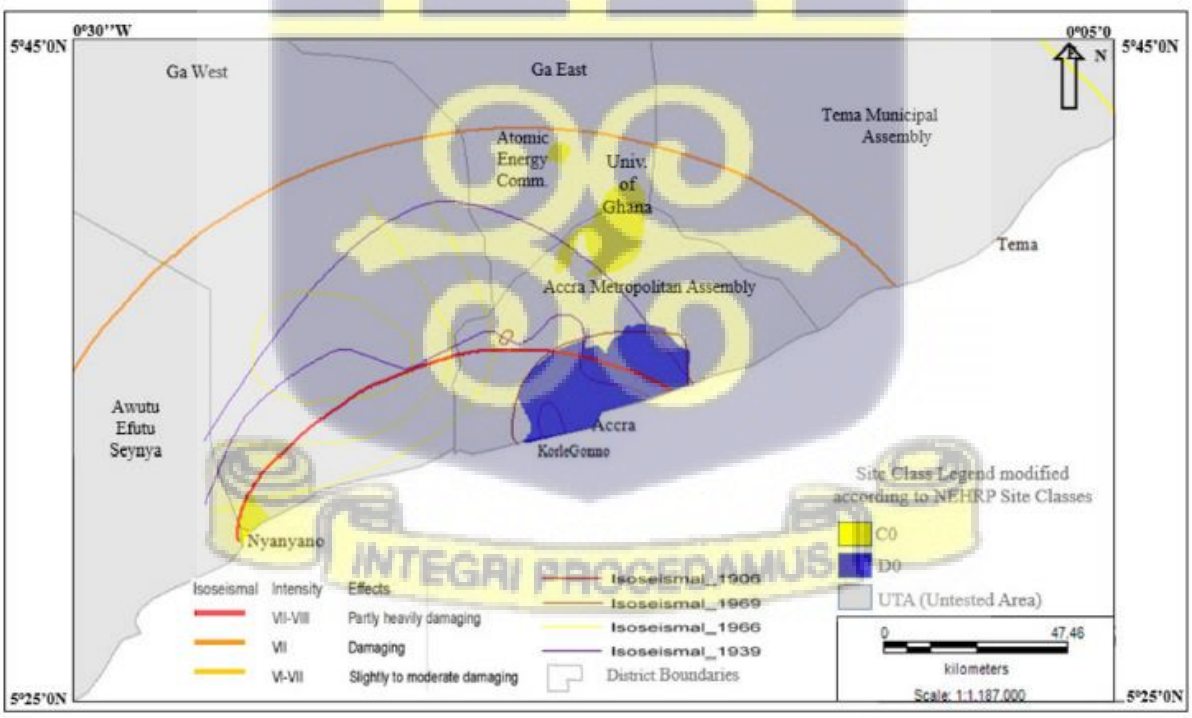

Figure 12 Site Classes C and D obtained with V_s^{30} analysis in some parts of the GAMA(Nortey et al., 2018)

Places to the west of Accra such as Nyanyano among others have shown significant high damage during previous earthquakes. However, the high shear wave velocity values obtained there did not conform to or follow the expected trend. The V_s^{30} values obtained may have been overestimated. Further studies into such areas will be needed to better understand and establish a solid correlation between the velocity and lithology of the area. As highlighted and believed by several authors, the knowledge of V_s^{30} alone is insufficient for structural and seismic risk assessment, the assumption that V_s increases with depth slightly differs due to varying soil deposition conditions which cause velocity inversions. Such areas can significantly affect the seismic energy propagating through them. Also in cases where a strong impedance contrast does not exist, $V_s^{30}$is not very accurate (Dikmen et al., 2015; Forte et al., 2019; Hunter et al., 2002; Pitilakis et al., 2018; Teague et al., 2018).

2.5 Earthquake Site Response in Accra

Ayetey & Andoh (1988) produced a seismic risk potential zone map using isoseismal lines VII and above (MMS) from the 22nd June 1939 earthquake as shown in Figure 13. The groupings into the zones were based on records of earthquake effects in the study area and the extent of damage by inspection. Areas in Category A – Maximum Damaged Zones were apportioned to areas on unconsolidated sand and clay deposits like Sakumo and Nyanyano and areas along the Togo series. This also included areas underlain by the Accraian in Accra. The greatest damage in this category was sited on underlying rocks of interbedded shales and sandstones particularly those covered by clay, sand, or a combination of these and other soils. Buildings on Accraian shales were damaged more than those on Accraian sandstones. In some areas, the study reports that the depth of the soft alluvium covering the Accraian played a major role in the structural damage recorded (Figure 13). The relationship between the period of vibration of structures and the period of vibration of the supporting soil influences the seismic behaviour of the soil-

structure system during an earthquake. Alluvium thickness is directly related to the period of vibration of the soil and hence can lead to great damage. Site response of different soils depends on the varying physical properties and depth variation and this leads to varying degrees of destruction to structures. Sands and clays that dominate the subsurface of Accra respond differently to earthquakes and hence a fairly different response is to be expected for different sites in Accra. The study pointed out that the isoseismal lines alone cannot be relied upon to reveal zones of high-risk potential and that bedrock topography, soil cover, surface topography, groundwater relationships, and numerous faults could subject several other places to a high risk of damage. Information on the periods of vibration of the weathered interbedded sands and shales of the study area will be needed to justify the engineering and physical properties of the subsoil as presented in the research.

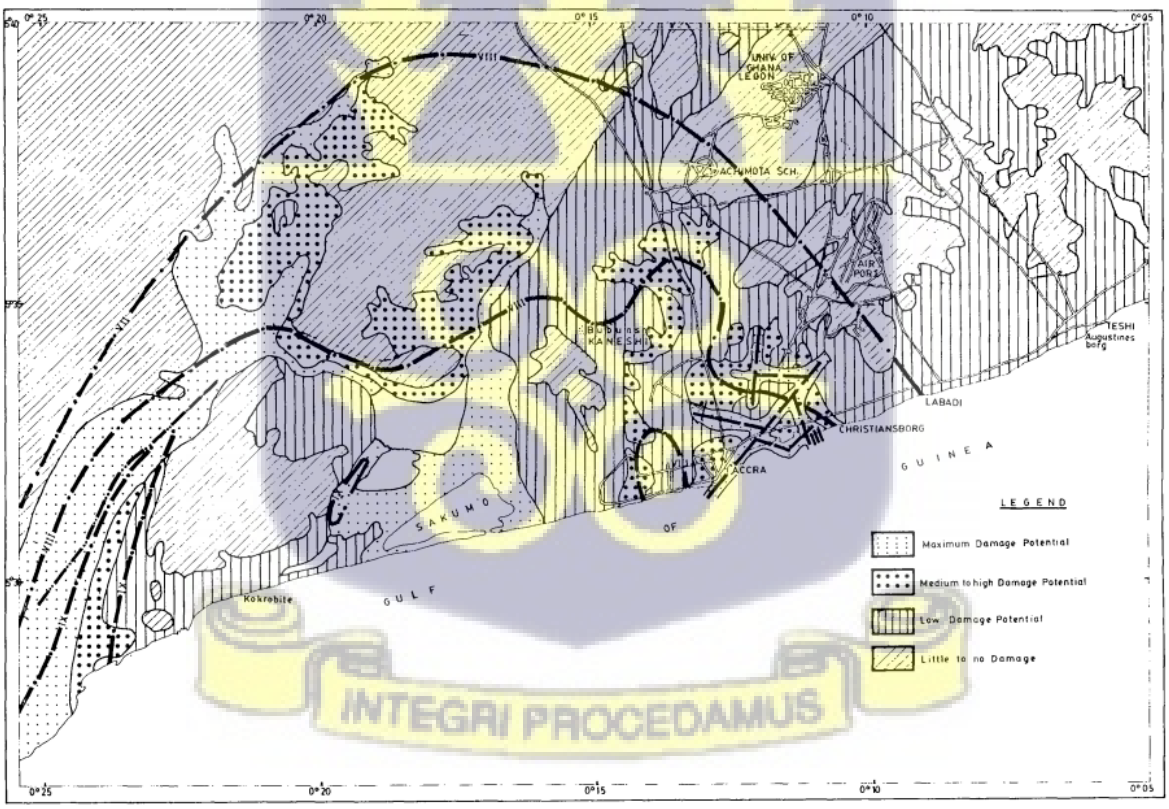

Figure 13 Earthquake risk potential zones of Accra using the 22nd June 1939 earthquake (Ayetey & Andoh, 1988).

2.6 Ambient Noise H/V Spectral Ratio Technique

The H/V spectral ratio method considers the fundamental resonance frequency characteristics of the soil as a function of geology (Onyebueke et al., 2017; Vella et al., 2013). It is site-specific and tells just how much the near-surface soft sediments amplify the earthquake ground motion. Above or at this threshold frequency, there may be significant amplification (Guéguen et al., 2000; Talha Qadri et al., 2015). Just like the $Vs30$, this method is also affected by the impedance contrast which shows the presence of an overlying soft sediment over stiffer bedrocks (Bonnefoy-Claudet et al., 2009; Guéguen et al., 2000; Parolai et al., 2004; Teague et al., 2018). The resonance frequency varies over short distances as it hugely depends on the sediment thickness and material properties (Paudyal et al.,2012). If the resonance frequency of the subsurface corresponds to that of the infrastructure seated on it, great damage will be recorded, even for small-magnitude earthquakes (Talha Qadri et al., 2015). This makes it an important parameter to investigate concerning site effects and micro zonation. In comparatively low seismic zones, where strong earthquakes occur rather rarely, the horizontal-to-vertical spectral ratio approach can be applied to ambient noise for site effect analysis to determine vulnerable zones effectively (Bahavar et al., 2020; Bonnefoy-Claudet et al., 2006b; Cadet et al., 2011; Talha Qadri et al., 2015).

2.6.1 Ambient Seismic Noise

The urgency for improved and reliable seismic risk assessment techniques mainly in urban centers has been a major concern for decades. Bonnefoy-Claudet, et al. (2006b) state that the numerous techniques employed to identify site response characteristics such as the resonance frequency and the amplification factor can be grouped into three main categories. The first method combines a numerical approach with the classical geophysical methods and tools like borehole logging, seismic refraction, and reflection methods amongst others to make reliable estimates (Panza et al., 2001). These techniques have several limitations in urban centres due

to cost concerns (Bonnefoy-Claudet et al., 2006b). Category two measures a direct and unbiased experimental estimate of the site response characteristics using earthquake recordings. The limitation of these techniques is that it is not as effective in moderate to low seismic areas (Bonnefoy-Claudet et al., 2006b). The final category is based on ambient noise recordings which is not affected by the limitations faced by the other categories. Ambient Seismic Noise has grown very popular in its importance and application to various fields including seismological investigations mainly because of its persistent and pervasive nature (Nakamura, 2000; Sens-Schönfelder & Brenguier, 2019). In comparison to coda waves, it is independent of the occurrence of earthquakes, and recording it has no restrictions as far as time and location are concerned (Bonnefoy-Claudet et al., 2006b; Janusz et al., 2022; Yang & Ritzwoller, 2008). It has therefore proven to be the most efficient, less time-consuming, and low-cost alternative method for estimating soil resonance frequency of urban centres all around the world (Talha Qadri et al., 2015; Bahavar et al., 2020; De Guevara et al., 2022). Ambient seismic noise is mainly composed of surface waves and therefore should have sources generating it from close to the Earth's surface (Stehly et al.,2006). Bonnefoy-Claudet et al. (2006b) highlighted that the frequency of ambient noise is dependent on its source. The sources may be natural such as tides, the force of waves striking the coast, effects of wind on buildings and trees. Cars, trains, huge machines, and even footsteps all contribute to ambient vibrations (Bonnefoy-Claudet et al., 2006a; Molnar et al., 2007a). Ambient noise occurs due to a large variety of sources and hence has a wide frequency range (0.02 Hz to 50 Hz). This characteristic allows it to be applied to explore depths of more than 100 m (Horike, 1985; Molnar et al., 2007a).

2.6.2 Fundamental Site Frequency and Fourier Transforms

When there exists a noticeable enough impedance contrast between layers in a layered site, the nature of waves propagating through them is changed significantly (Talha Qadri et al., 2015).

The propagating waves through the site can also be significantly amplified if their frequency matches the fundamental site frequency (Abdel-Rahman et al., 2012; Gospe et al., 2020; Ranjan, 2005). The main focus of most seismic hazard analyses is to investigate the degree and magnitude of change offered to the propagating wave by soft sediments concerning hard rock underneath (Hunter et al., 2002; Talha Qadri et al., 2015). At two different depth levels, the ratio of the Fourier amplitude spectra for the two depths provides the Empirical transfer functions of the site (Teague et al., 2018; Van Ginkel et al., 2022). The Fourier transforms are used to convert the time domain signal recordings to the frequency domain where the complex signal is broken down to allow identification of dominant frequencies (Shatkay, 1995). These dominant frequencies correspond to the fundamental site frequency of the ground. Knowledge of the fundamental site frequency is critical for assessing potential seismic hazards to structures in the area.

2.6.3 Horizontal / Vertical Spectral Ratio (HVSR)

The horizontal-to-vertical spectral ratio method has been shown by a lot of researchers to be capable of identifying the fundamental resonance frequency and to an extent the amplification factor of sediments (Bonnefoy-Claudet et al., 2006a, 2006b; De Guevara et al., 2022; Field & Jacob, 1993; Horike, 1985; Konno & Ohmachi, 1998; Molnar et al., 2007a; Nakamura, 2000; Parolai et al., 2004; Talha Qadri et al., 2015). Also known as the Nakamura method, it is based on a few assumptions which he highlighted in his 1989 publication. The microtremors observed at the surface are considered to be composed of both body and surface waves with unclear proportions and this leads to one of the assumptions of the method which suggests that the surface waves are mainly composed of Rayleigh waves. According to Bonnefoy-Claudet et al. (2006b) several authors have attributed the surface waves of microtremors to be mainly due to Rayleigh waves. Other articles have also shown that the peak period obtained using the HVSR of microtremors is related to that obtained when using the Fundamental-Mode Rayleigh waves

(Konno & Ohmachi, 1998; Lermo & Chavez-Garcia, 1993; Mulargia & Castellaro, 2016; Piña-Flores et al., 2020). One other assumption of the method is that the amplification effect comes about because the ground is layered and there is a soft sediment layer covering a rocky hard layer (De Guevara et al., 2022; Suhendra et al., 2018; Talha Qadri et al., 2015; Ullah & Prado, 2017).

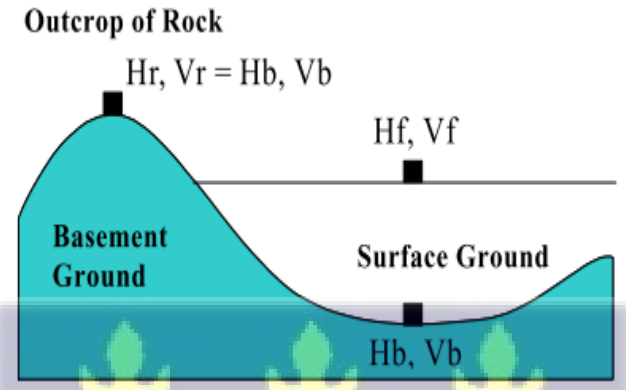

Figure 14 A typical geological structure based on the Nakamura technique (Nakamura, 2000; Onyebueke et al., 2017)

Figure 14 demonstrates a typical sedimentary basin as used in the assumptions of Nakamura (2000). Four motion components' amplitude spectra are taken into account in these circumstances; two components of motion for both vertical and horizontal components are captured in the rock and on the surface (H_f, V_f, H_b, V_b). The ratio of horizontal motion at the surface to the bedrock can be used to assess the amplification properties of the horizontal motions; this relates to the site effect (H_f/H_b) and is of earthquake engineering interest (De Guevara et al., 2022; Lermo & Chavez-Garcia, 1993). It is, however, difficult to determine the resonance frequency for the surface layer considering just this because the spectra reveal several peaks. The several peaks result from microtremors consisting of several surface waves which influence the spectra (De Guevara et al., 2022; Molnar et al., 2007a; Nakamura, 2000, 2019). Since Rayleigh waves are thought to have strong vertical component motion, the ratio of vertical motion at the surface and bedrock (V_f/V_b) reduces the influence of Rayleigh waves

and is related to the amplitude effect of the source (De Guevara et al., 2022; Lermo & Chavez-Garcia, 1993). A modified site effect function which emphasizes the effects of several horizontally polarizing shear wave (SH) reflections, and reduced peaks caused by Rayleigh waves can be obtained by dividing H_f/H_b by V_f/V_b (De Guevara et al., 2022; Molnar et al., 2007a; Nakamura, 2000, 2019). P-wave velocity is generally faster than the SH (shear horizontal) wave and hence travels through the surface in a comparatively shorter time. There is essentially less to no amplification caused by the layers of *P*-waves at the resonance frequency of the *SH*-waves; in effect, vertical component motion cannot be amplified at the frequency band where the horizontal component is amplified significantly (Nakamura, 2000, 2019; Rošer & Gosar, 2010). This makes significant alteration to the modified site effect function as the ratio of vertical motions between the surface layer and the bedrock approximates unity in the said frequency band. The modified site effect function now takes the form H_s/V_s; the horizontal-to-vertical spectral ratio is also known as the Nakamura ratio. The spectra reveal a stable peak which is the fundamental site frequency. For HVSR, microtremors are recorded with a three-component seismometer; two orthogonal horizontal components (North-South and East-West) and one vertical component (De Guevara et al., 2022; Molnar et al., 2007a; Parolai et al., 2004; Rošer & Gosar, 2010; Tanjung et al., 2021).

2.6.4 Sedimentary Thickness

Nakamura, through boring surveys, established a relation between the average shear-wave velocity of the soft surface layer (V_s), the thickness (h), and the fundamental resonance frequency (f), ($f = V_s/4h$)(Nakamura, 2000, 2019; Rošer & Gosar, 2010; Tanjung et al., 2021; Tian et al., 2019). Seht & Wohlenberg (1999) used a nonlinear regression model to arrive at an equation that shows that the fundamental site frequency (f) of a surface layer is directly related to its thickness (h); $h = af^b$ where a and b are adjustable correlation coefficients.

2.6.5 Vulnerability Index (K_g-values)

Earthquake damage depends on the strength, period, and duration of seismic motions (Nakamura, 1996). These parameters, however, are to a large extent influenced by subsurface characteristics as well as structures (Nakamura, 1996, 2000, 2019). Problematic sites as has been described, need to be identified with great urgency. Site investigations that lead to such inference need to be simple and fast but also consistent with other methods, especially in urban areas. A different parameter; the fragility index of the ground K_g (vulnerability index) has been proposed to evaluate the risk of liquefaction using HVSR (Nakamura, 2000). The passage of seismic waves through the subsurface may distort the structure of sediments. Loosely-packed soils may lose their strength during an earthquake and start to flow like a liquid, this process is known as liquefaction (Moustafa et al., 2022). Vulnerable and weak sites can be identified by examining seismic waves and their behaviour as they travel through the surface and even structures (Moustafa et al., 2022; Nakamura, 1996, 2000, 2019; Suhendra et al., 2018). In recent years, several reports have shown a good correlation between K_g values and earthquake damage (Moustafa et al., 2022; Nakamura, 1996, 1997). K_g of the surface ground and structures are obtained by considering shear strain (Huang & Tseng, 2002; Moustafa et al., 2022; Nakamura, 1996, 1997). The equation obtained for K_g is; $K_g = A_o^2/f_o$; where A_o and f_o represent respectively the peak amplification and fundamental site frequency (resonance frequency) obtained through the Nakamura ratio (Huang & Tseng, 2002; Moustafa et al., 2022; Nakamura, 1996, 1997, 2000, 2019; Suhendra et al., 2018; Tanjung et al., 2021).

2.6.6 Site-response zonation map

The parameters of the various sites; resonance frequency f_o and its corresponding amplification factor A_o and the vulnerability index K_g are used to generate a site response zonation map for further analysis. For areas within the selected area where V_s measurements exist, the sedimentary thickness can be estimated to help in further analysis.

This method has been used in the urban city of Fateh Jang in Pakistan by Talha Quadri et al. (2015) to analyze site response to earthquakes. The important local site parameters; fundamental frequency, f_0, the amplitudes of the corresponding H/V spectral ratios, A_0, and thickness were determined for 13 sites in the area. After the analysis, it was inferred that the site had a relatively low fundamental frequency ranging from $0.6 - 13.0\,Hz$. The corresponding H/V spectral ratio amplitudes also ranged from $2.0 - 4.0$. The depth to bedrock was also extremely variable and ranged between $2.20\,to\,238.50$ meters. The guidelines described by SESAME (2004) were used to check the reliability of each of the 13 stations of which none failed. The low fundamental frequency and correspondingly greater alluvium thickness indicate a high seismic risk following the possible amplification that the site can pose to seismic waves. This information correlates with previous risk assessments conducted in the area and is very useful to policymakers and disaster management authorities. Well-informed mitigation strategies can now be devised in a bid to reduce future disasters.

Onyebueke et al. (2017), employed the very reliable, cheap, and easy HVSR technique to access site effect characteristics of the topsoil in some areas in South Africa by deducing the fundamental frequency of the ground motion. The values from the stations that satisfied the H/V peak criteria according to the SESAME (2004) were used to estimate the thickness of the sedimentary cover and the vulnerability index. The fundamental frequency and amplification values ranged from $0.45 - 18.10\,Hz$ and $1.10 - 3.13$ respectively. The most vulnerable zones according to the method were those that showed low to high peak frequency values that ranged from $0.94 - 9.41\,Hz$ and amplitudes $1.58 - 3.13$ belonging to sites situated on alluvial sand, superficial deposits, and highly weathered surfaces, being most likely to amplify the ground motion. Sites situated on hard rocks showed flat H/V curves with low amplification factors of $1.10 - 1.33$. The fundamental frequency was also determined for data from the same site but

different times and seasons. This showed little to no variation, indicating that the parameter does not depend on time and season.

De Guevara et al. (2022) researched to determine whether future construction works should consider soil characteristics in La Mesa de Macaracas, Panama. For 16 stations, measurements of ambient vibrations were made, analyzed, and used to determine the fundamental frequency and corresponding H/V ratio peaks. Class I consist of medium and hard soils. These soils recorded high predominant frequencies and lower spectral ratio values, indicating low amplification. Class II consists of soft sediments. These sediments were characterized by lower predominant frequencies and higher spectral ratio values, indicating high amplification. For future constructions, the research concluded that resonance could affect 3 to 5 storeys in the medium and hard rocks while in soft rocks, resonance will affect 6 to 14 storeys. The results obtained are very useful for civil engineering and structural analysis to inform on the choice of materials, site, and the general design of new construction works.

CHAPTER THREE
METHOD

3.1 Data Acquisition and Analysis

The current study was carried out by collecting ambient noise from 14 different data points using the *Taurus Trillium Nanometric* as shown in Figure 15. The Trillium seismometer was placed in a stable and secure location on the ground at each site to achieve effective soil-to-sensor connections for each reading and away from any artificial vibrations like heavy machinery. The ground was cleared of debris, vegetation, and any loose material. The three adjustable height feet and the levelling bubble work together to level and centre the sensor precisely. Proper alignment was also ensured by positioning the sensor such that the north-south vertically scribed marks and the north-south case-top guide all point in the direction of the North using a compass (Figure 16). The system's clock was then synchronized with GPS time. After this, the seismometer was protected from adverse weather conditions such as extreme temperature or rain using the insulated seismometer cover (Figure 15). A continual recording of ambient noise for about 10 to 20 minutes at a sample rate of 100 Hz was made taking into account the guidelines from the SESAME project (Marcellini, 2006). The GEOPSY software was used to process the data and calculate the h/v ratio after the recordings were downloaded from the seismometer. The ambient noise recordings are then imported into the software and reviewed for any obvious issues such as gaps, spikes, or periods of non-seismic noise to ensure good data quality. The orientations of the components (N-S, E-W, Z) are also reviewed to ensure that they are correctly recognized by the software As shown in Figure 17, the recordings were then divided into low-noise 25-second windows using the short-term average (STA)/ long-term average (LTA) anti-trigger. STA was given a value of 2 s while LTA was given a value of 30 s with min STA/LTA and max STA/LTA thresholds of 0.2 and 2.5 respectively. Cosine taper is applied at two ends of the selected signal window while processing ambient noise recording to overcome abrupt discontinuities that greatly affect the Fourier

spectrum (Chatelain & Guillier, 2013). Konno-Ohmaci smoothing option was applied to smoothen the Fourier amplitude spectra along with the Cosine taper. The 'squared average' option was used to combine the Fourier spectra of the horizontal components (Figure 17). These processing procedures were completed following the instructions in the Geopsy manual (Wathelet et al., 2020). The H/V is finally determined and the fundamental frequency, f_o and its corresponding amplification factor, A_o are deduced from it. Data reliability was checked based on the conditions proposed by Marcellini (2006) which includes $f_o > 10/L_w$, $n_c\,(f_o) > 200$, (where $n_c = n_w \times L_w \times f_o$) and $A_o > 2$ (l_w = window length, f_o = H/V peak frequency, n_w = the number of windows selected for the average H/V curve, n_c = the number of significant cycles, A_o = H/V peak amplitude at frequency f_o). The parameters are then used to estimate the thickness H of the sedimentary layer and the vulnerability index of the site. To show spatial variation of the results, interpolation by the Inverse Distance Weighted method was applied through the ArcGIS software. This was done by first importing a tabulation of the results with columns for coordinates into the ArcGIS software. These measurements were georeferenced. Separate interpolated surfaces were generated for the resonance frequency, amplification factor, sedimentary thickness and the vulnerability index.

Figure 15 Taurus Trillium Nanometric. (1) Nanometric Trillium seismometer (2) Insulating seismometer base (3) Insulated seismometer cover (4) GPS antenna (5) Nanometric Taurus datalogger (6) battery

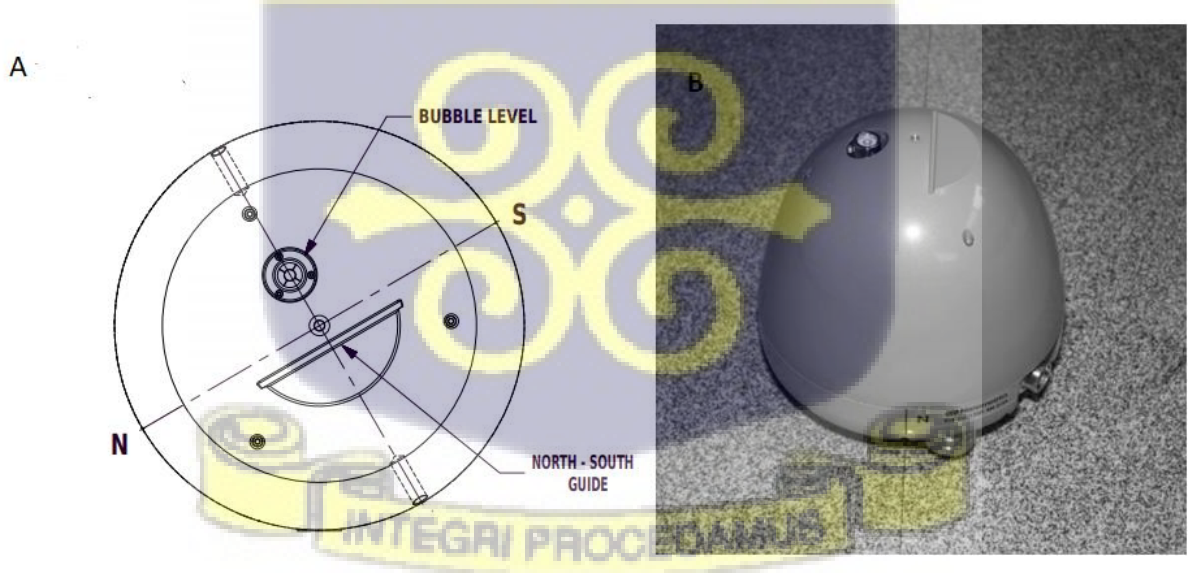

Figure 16 (A) Top view of the Trillium sensor showing the various alignment and leveling features; bubble level, north-south scribed vertical lines, and case-top guide (B) An illustration of the north-south scribed vertical being aligned to a north-south trending line. On the field, a compass is used.

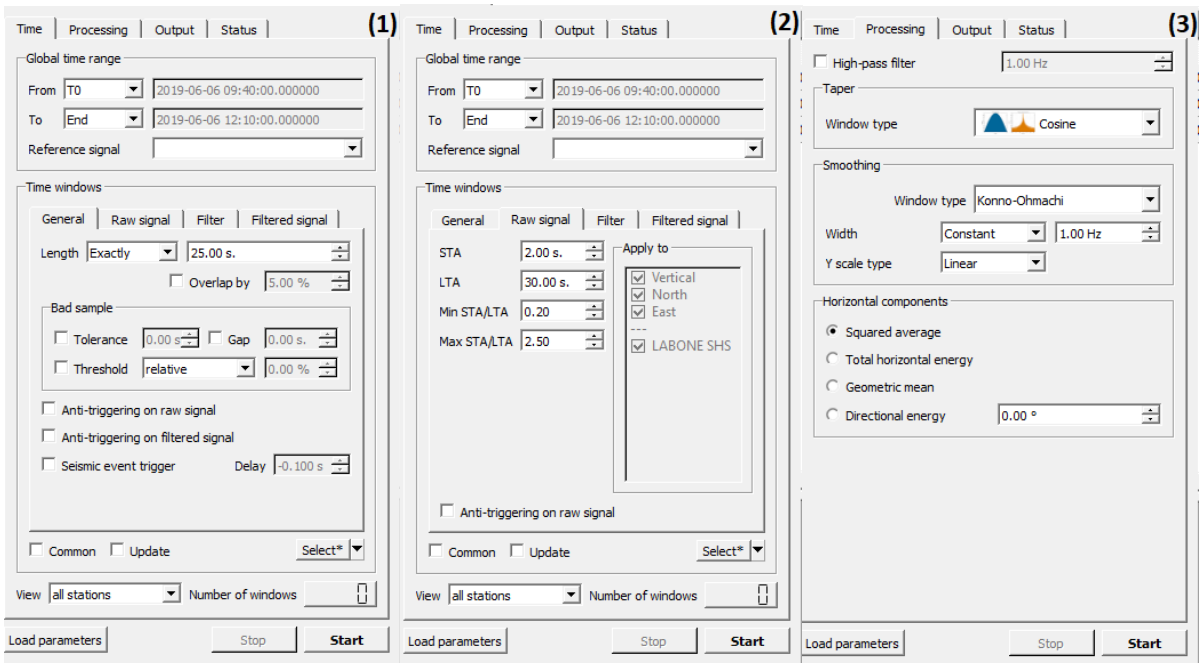

Figure 17 Signal Processing using the GEOPSY software.

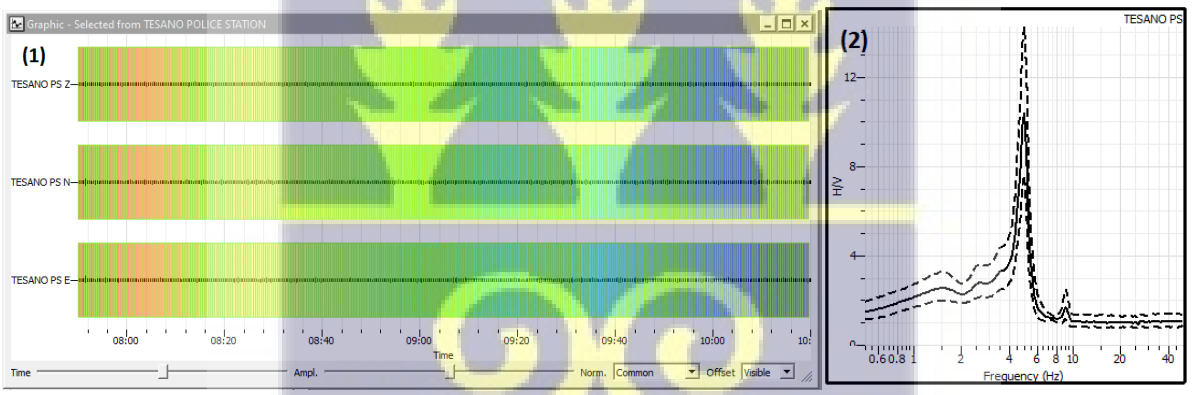

Figure 18 (1) Window selection for three components of the ambient recordings. (2)A sample of the h/v curve after the processing

CHAPTER FOUR

RESULTS AND DISCUSSIONS

The horizontal-to-vertical spectral ratio analysis has been computed from ambient noise recordings for the 13 sites. Table 2 represents the results obtained for the fundamental site frequency and its corresponding amplification factor as well as the data reliability check as proposed by the SESAME project (Marcellini, 2006). The reading from Aburi was rendered unreliable because the amplification factor is less than 2. Table 3 shows the estimations of sedimentary thickness, H and the vulnerability index, K_g of each site from Table 2.

Table 2 Reliability of frequency peaks/curves based on parameters defined by guidelines modified by (Marcellini, 2006)

Station	Lat	Long	f_o	$A_o > 2$	$f_o > 10/l_w$	n_w	$n_c(f_o) > 200 = n_w \times l_w \times f_o$	Comment
Aburi	5.84	-0.18	0.73	1.66	0.4	23	420.06	UNRELIABLE
Anyaa DL	5.59	-0.29	6.75	3.13	0.4	23	3882.71	RELIABLE
Ayikuma	5.77	-0.18	11.00	2.34	0.4	23	6328.22	RELIABLE
LA	5.58	-0.16	4.06	2.17	0.4	23	2331.62	RELIABLE
C&W								
Labone	5.56	-0.16	9.40	2.90	0.4	23	5404.31	RELIABLE
SHS								
Lapaz	5.61	-0.25	11.02	2.02	0.4	23	6335.01	RELIABLE
NADMO	5.58	-0.19	5.49	2.20	0.4	23	3156.08	RELIABLE
HO								
N-LN	5.69	-0.16	8.47	2.70	0.4	23	4869.84	RELIABLE
Bus								
Terminal								
Odorkor	5.58	-0.26	10.12	2.06	0.4	23	5819.86	RELIABLE
SDA								
Otinshiie	5.66	-0.15	6.44	3.11	0.4	23	3703.56	RELIABLE
Pantang	5.72	-0.19	7.33	2.49	0.4	23	4212.80	RELIABLE
HOSP.								
Social	5.68	-0.16	7.79	2.023	0.4	23	4483.46	RELIABLE
Welfare								

Tesano PS	5.60	-0.22	4.95	9.94	0.4	23	2850.06	RELIABLE

Table 3 13 sites of data acquisition along with corresponding fundamental frequencies f_o, amplification factors A_o, thicknesses H and the vulnerability index K_g.

Station	Latitude	Longitude	f_o	A_o	H	$K_g(A_o^2/f_o)$
Aburi	5.84	-0.18	0.73	1.66	175.75	3.81
Anyaa DL	5.59	-0.29	6.75	3.13	5.58	1.45
Ayikuma	5.77	-0.18	11.00	2.34	2.62	0.49
LA C&W	5.58	-0.16	4.06	2.17	12.31	1.16
Labone SHS	5.56	-0.16	9.40	2.90	3.34	0.87
Lapaz	5.61	-0.25	11.02	2.02	2.61	0.37
NADMO, HO	5.58	-0.19	5.49	2.20	7.69	0.88
N-LN Bus Terminal	5.69	-0.16	8.47	2.70	3.92	0.84
Odorkor SDA	5.58	-0.26	10.12	2.06	2.98	0.42
Otinshiie	5.66	-0.145	6.44	3.11	6.00	1.50
Pantang HOSP.	5.72	-0.19	7.33	2.49	4.91	0.84
Social Welfare	5.67	-0.16	7.79	2.03	4.46	0.52
Tesano PS	5.60	-0.22	4.95	9.94	9.02	20.00

4.1 Fundamental site frequency f_o and Alluvium thickness estimates

The fundamental site frequency values obtained after the analysis of the recordings from the 13 sites are shown in Table 3. The values ranged from 0.73 Hz to 11.00 Hz. The thickness over the area also ranged from 2.61 m to 175.75 m. The least fundamental site frequency value occurred

at Aburi with a value of 0.73 Hz, while Lapaz recorded the highest value of 11.02 Hz. The highest f_o corresponds with the lowest thickness and the lowest f_o corresponds to the highest thickness.

4.2 Amplification factor A_o and Alluvium thickness estimates

The amplification factor from the HVSR analysis ranges from 1.6 to 10.0. The least amplification recorded corresponds to the highest alluvium thickness. The highest estimated amplification factor, however, does not correspond to the maximum alluvium thickness. The thickness estimated at Tesano PS is 9.00 $meters$ which is comparatively deep (Table 3).

4.3 Vulnerability Index, K_g $({A_o}^2/K_g)$

The values from the estimation of the vulnerability indices range from 0.37 to 20.00. Tesano PS showed the highest reading of 20.00. Lapaz recorded the lowest value of 0.37 (Table 3).

4.4 Implications of H/V curves and f_o concerning site characteristics

Most instances in Literature indicate that H/V curves for soft soils have noticeable peaks while rocky sites appear nearly flat (Bonnefoy-Claudet et al., 2009; Bour et al., 1998; Fäh et al., 1997; Lermo & Chavez-Garcia, 1993). The presence of peaks suggests the possibility of amplification of seismic ground motion. The height of the peak indicates the degree of amplification of the ground motion at the corresponding resonance frequency (Lermo & Chavez-Garcia, 1993). The curves obtained during the study include clear single peaks, multiple peaks, flat peaks, and broad peaks as shown in Figure 19 and Figure 20.

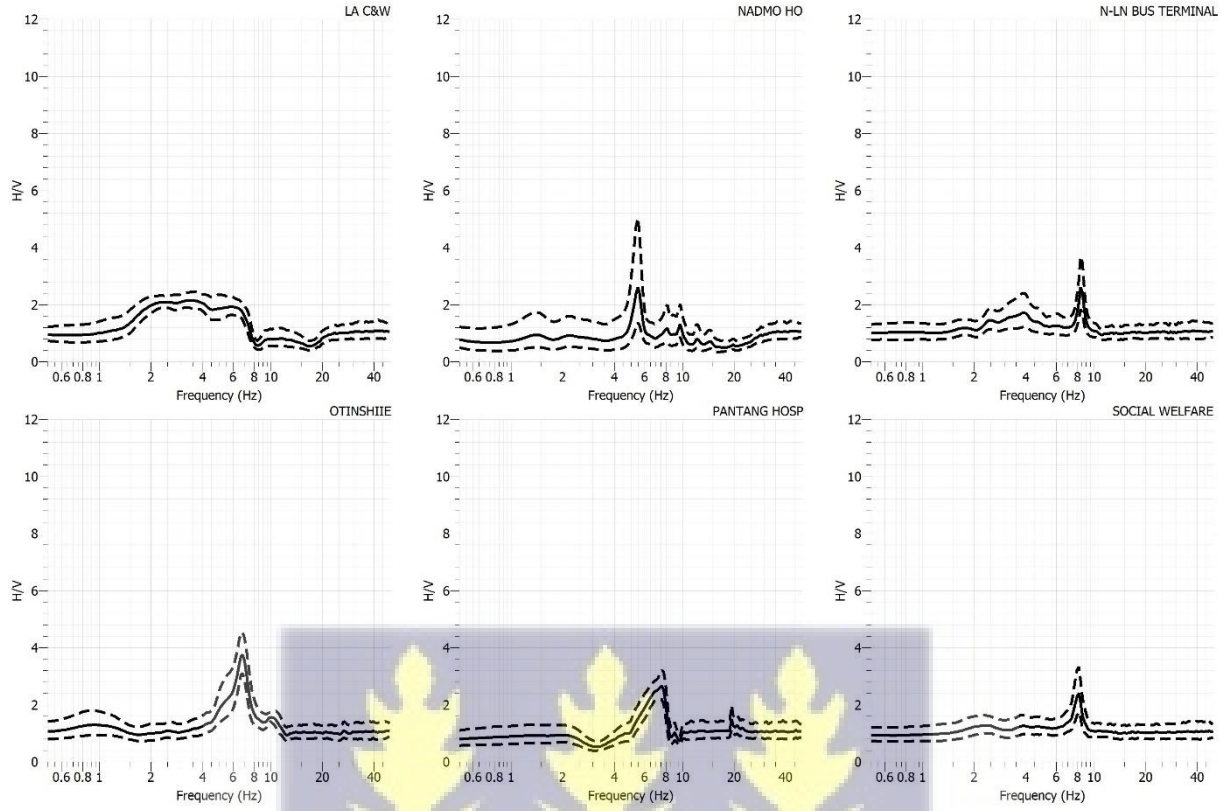

Figure 19 H/V curves for the various sites

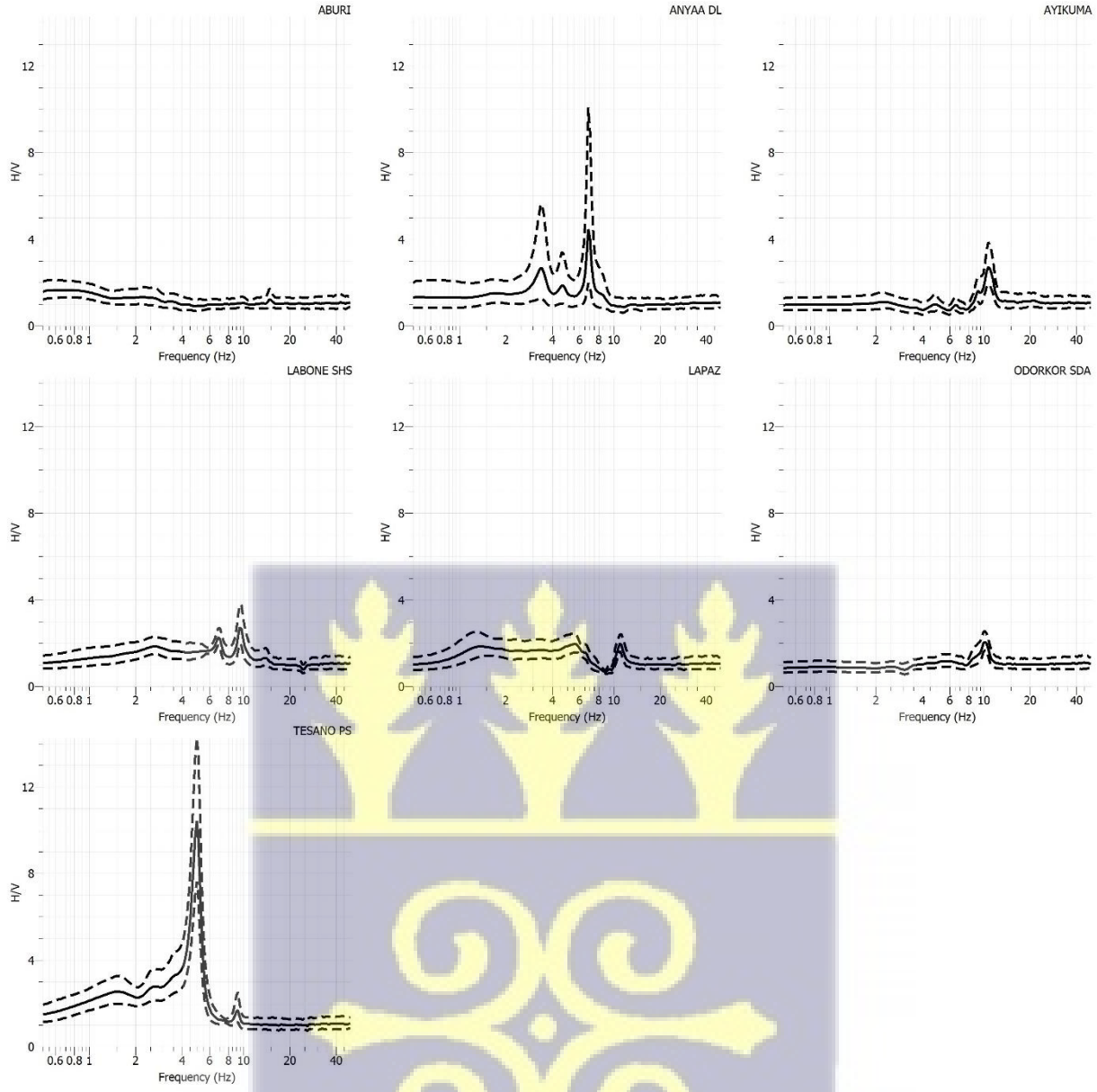

Figure 20 H/V curves for the various sites

4.4.1 Clear Peaks

Clear and distinct curves correspond to the natural frequencies of the subsurface layers. A clear single peak has been exhibited in some sites such as the ones labeled Tesano PS and Otinshie among others as shown in Figure 19 and Figure 20. Such curves may be an indication of a single layer that presents a large impedance contrast and is usually likely to amplify ground motion. Higher peaks correspond to higher velocities, which may signify softer soils overlying a more rigid or denser rock (Bonnefoy-Claudet et al., 2009; Cruz et al., 1993; SESAME, 2004). According to Bonnefoy-Claudet et al. (2009) and Lermo & Chavez-Garcia (1993), softer and less dense materials tend to have lower resonance frequencies and corresponding higher amplification, while stiffer and denser materials have higher resonance frequencies and lower amplification. Tesano PS appears to be the most vulnerable according to this analysis.

4.4.2 Multiple Peaks

The presence of multiple clear peaks may be an indication of the presence of multiple surface layers with varying shear wave velocities. Each peak represents the fundamental frequency of the distinct geotechnical layers (Lermo & Chavez-Garcia, 1993). The curve from Anyaa DL shows the most prominent double peaks (Figure 20).

4.4.3 Broad Peaks

Broad peaks may also be an indication of multiple layers with slightly different fundamental frequencies. It may also be an indication that amplification may occur over a large range of frequencies which are less distinct than the sharp multiple peaks(Lermo & Chavez-Garcia, 1993). LA C&W demonstrated a broad peak (Figure 19).

4.4.4 Flat Curves

A flat curve may reflect a consistent site response that is less susceptible to amplification or resonance effects, it is typically regarded as being advantageous for seismic resilience. Flat curves may be due to a lack of resonance that suggests that there is an absence of an impedance contrast. It also suggests that the site is on solid bedrock. In effect, a uniform layer of soil extends over a range of depths(Lermo & Chavez-Garcia, 1993; SESAME, 2004). Aburi shows a flat curve (Figure 20).

4.5 Characteristic response of different lithologies

The different lithologies appear to show varying responses to seismic motion based on their H/V curves. In Figure 21, the spatial variation of f_o and A_o has been shown on a map of the basement rocks of the GAMA. The length of the bars indicates the magnitude of the fundamental frequency and amplification factor recorded at the site. The site of most interest is the Tesano PS which appears to be the most vulnerable because it has a smaller fundamental frequency but high corresponding amplification indicating soft soils. Its H/V curve peak also supports this (Figure 20). Also, in Figure 23, the site in Tesano PS is on clayey sands.

The site in Aburi shows both the lowest fundamental frequencies and corresponding amplification. Since the curve and values correspond to a zero-impedance contrast site, further analysis suggests that the ambient noise recording at that site might have been made on a hard outcrop which could be a basement rock on a high ground (Figure 22). Ayikuma is located just at the transition between the Togo and the Dahomain, and considering the contours, it appears to be on a relatively lower land. This may be the reason for the difference in site response there as there may be some settled shallow weathered rocks overlying the basement rock. Anyaa DL differs as its curve demonstrates distinct peaks suggesting a complex soil combination. In a modified residual soil map of some

parts of the GAMA, it is sited on a high quarzitic gravelly laterite. The H/V curve in Figure 20 confirms this.

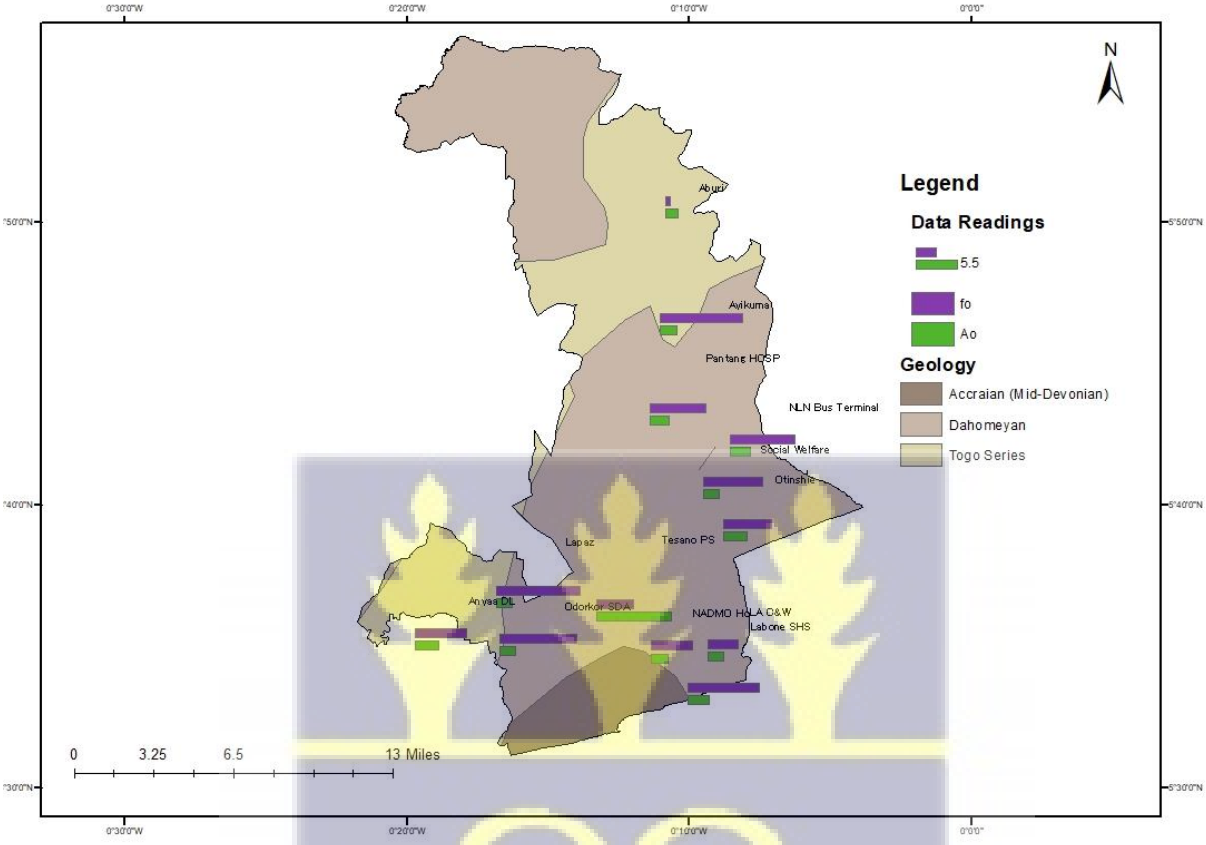

Figure 21 Site Response Map for selected sites in the GAMA.

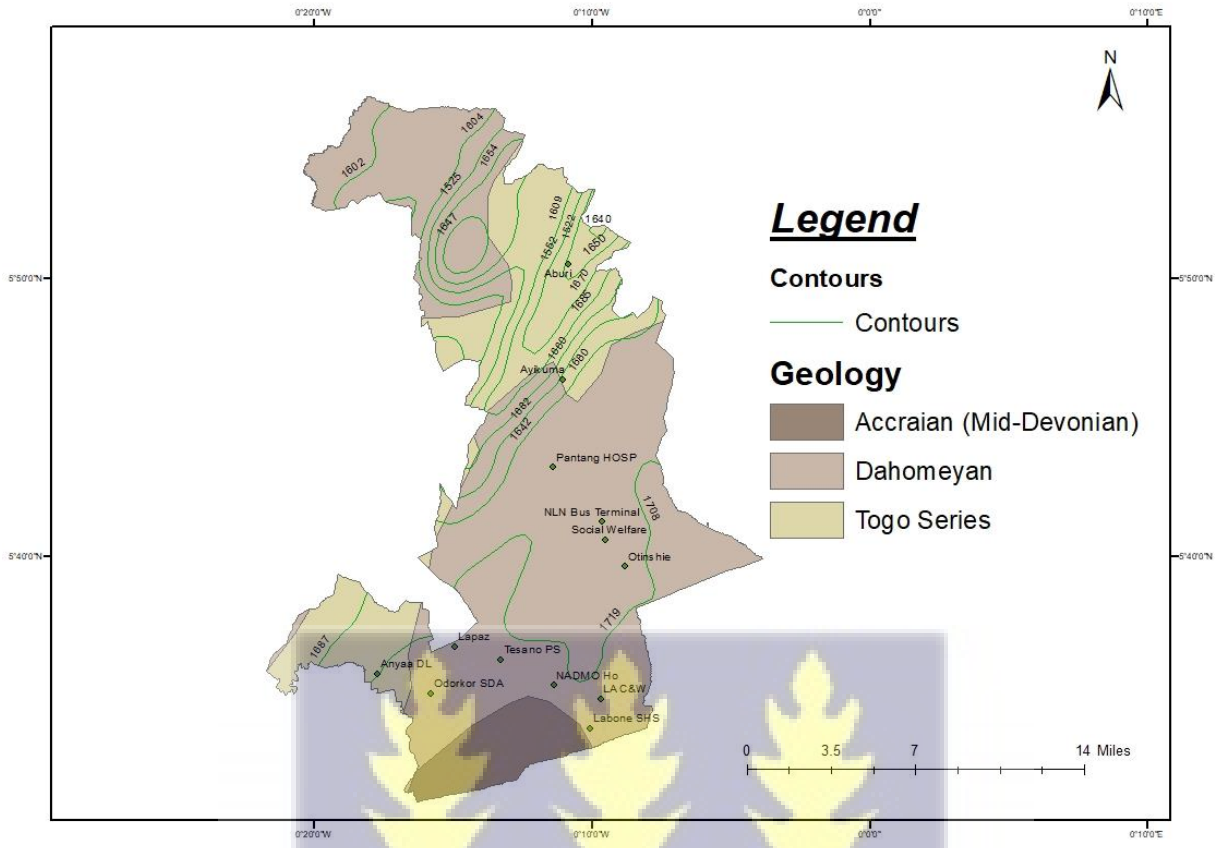

Figure 22 Site Response Map for selected sites in the GAMA showing contours

Most sites are distributed in the Dahomeyan, and areas distributed in the central part of the lower Dahomeyan recorded values within a close range. Pantang HOSP, NLN Bus terminal, Social Welfare, and Otinshie have close fundamental sites and their corresponding amplification. In Figure 19, they all show similar curves.

Odorkor SDA, NADMO Ho, Lapaz, LA C&W, and Labone SHS sites show some complexities with varying curves. Odorkor SDA and the Lapaz site showed almost similar curves and close values. They are both found on the earthy laterite which is clayey with little gravel in general. The site from NADMO Ho produced a single distinct peak with smaller peaks, in Figure 23 it is at the transition between highly quarzitic gravelly laterite and sandy clay. It may contain soils from both sides and that explains the peaks on the curve (Figure 19). LA C&W is located also on highly

quarzitic gravelly laterite but produced a broad peaked curve suggesting multiple layers of close fundamental frequencies. Labone SHS site may contain residual soils from the clayey sands and sandy clays resulting in small but distinct peaks on the curve.

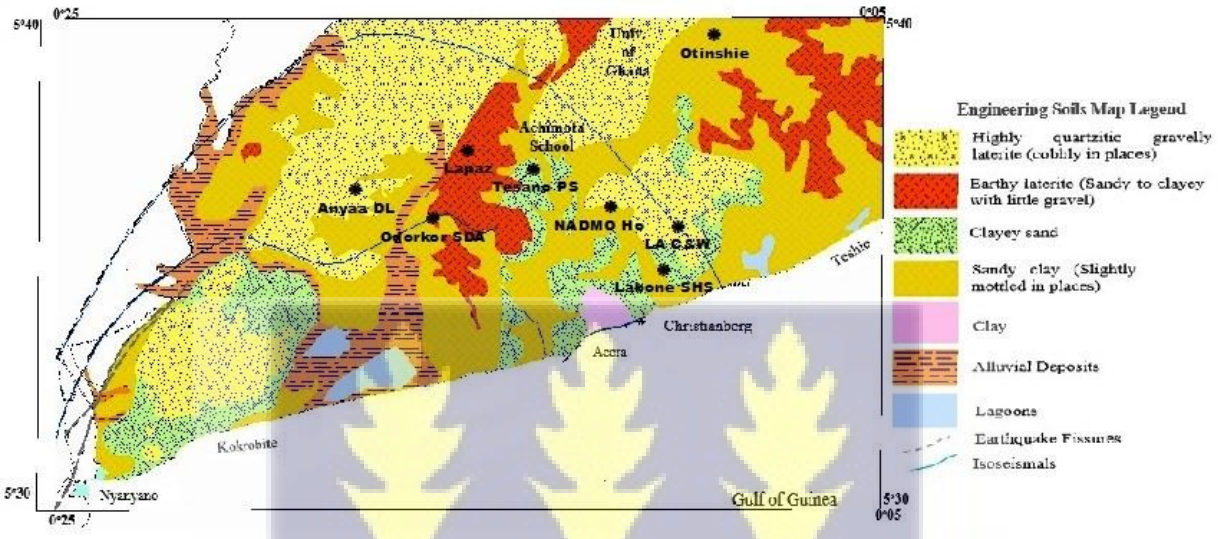

Figure 23 Engineering soils of some parts of the GAMA where data was recorded (modified after Nortey et al., 2018*)*

4.5 Implication of vulnerability index K_g values

The vulnerability index estimate is an important parameter that is employed to calculate the levels of rock solidity and rock structure characteristics (Huang & Tseng, 2002). Areas with high values are considered to have weak structures and hence soft soils. During earthquakes, such soils can be moved easily by the shaking. Tesano PS recorded the highest value and may be susceptible to high damage during earthquakes. Aburi recorded the second-highest K_g value, but on highlands and along roadsides, such values show a risk of landslides and liquefaction.

4.6 Interpolation of obtained parameters

The spatial extent of the parameters from Table 3 was obtained using the Inverse Distance Weighted (IDW) method from the ArcMap software. The study area has been divided into three different zones in terms of fundamental frequency f_o, amplification factor, A_0, sedimentary thickness, H, vulnerability fact, Kg.

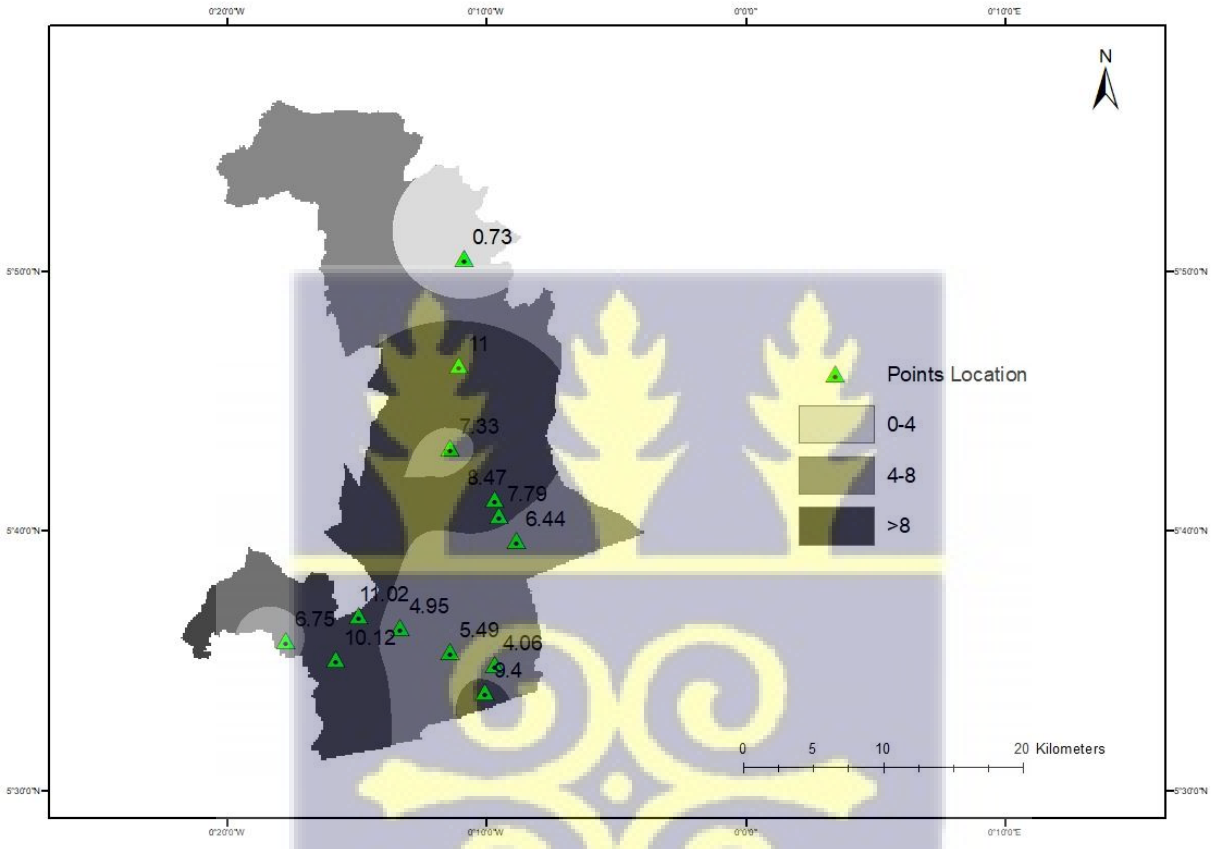

Figure 24 Interpolated map representing fundamental frequency, fo, for the study area

Zone 1 (grey) shows the lowest fundamental frequency values ranging from 0 – 4.0 Hz. Zone 2 shows mostly intermediate fundamental frequency values ranging from 4.0 – 8.0 Hz. Zone 3 (darker shade) shows the highest fundamental frequency values greater than 8.0 Hz represented by the dark grey shade. The distribution of fundamental frequencies can inform building design and construction practices. Engineers and urban planners might use this information to design

structures with natural frequencies that avoid resonance with the local ground frequency, thereby reducing the risk of damage. Buildings in areas with fundamental frequencies matching their natural frequencies should be targeted first for upgrades to improve their resilience. Understanding the distribution of fundamental frequencies can assist in emergency response planning by highlighting areas where damage might be more severe in the event of an earthquake.

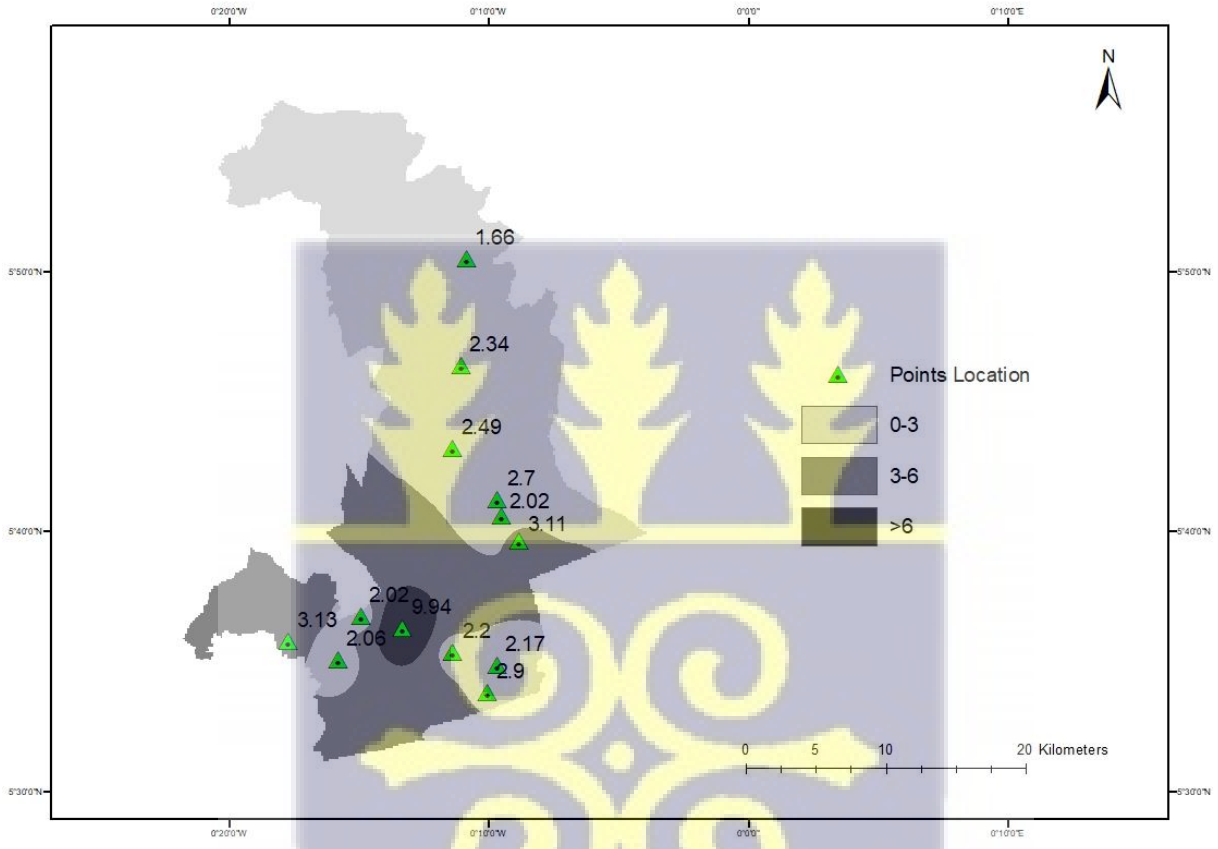

Figure 25 Interpolated map representing the amplification factor, Ao, for the study area

Zone 1(grey) has the lowest amplification factor values ranging from 0 – 3.0. Zone 2 has mostly intermediate amplification factor values ranging from 3.0 – 6.0 *Hz*. Zone 3 (darker shade) has the highest amplification factor values greater than 6.0 represented by the dark grey shade around the Tesano PS site. The map highlights that this zone has the highest amplification factor and should be flagged for further investigation or mitigation strategies. Buildings in areas with high

amplification factors are more likely to suffer significant damage, especially if they are not designed to withstand increased shaking. Areas in high amplification zones may require stricter building codes to ensure that structures are designed to withstand potential resonance effects. The map can also assist in emergency response planning. Knowing which areas will likely experience the most shaking can help prioritize evacuation routes, emergency services, and resource allocation.

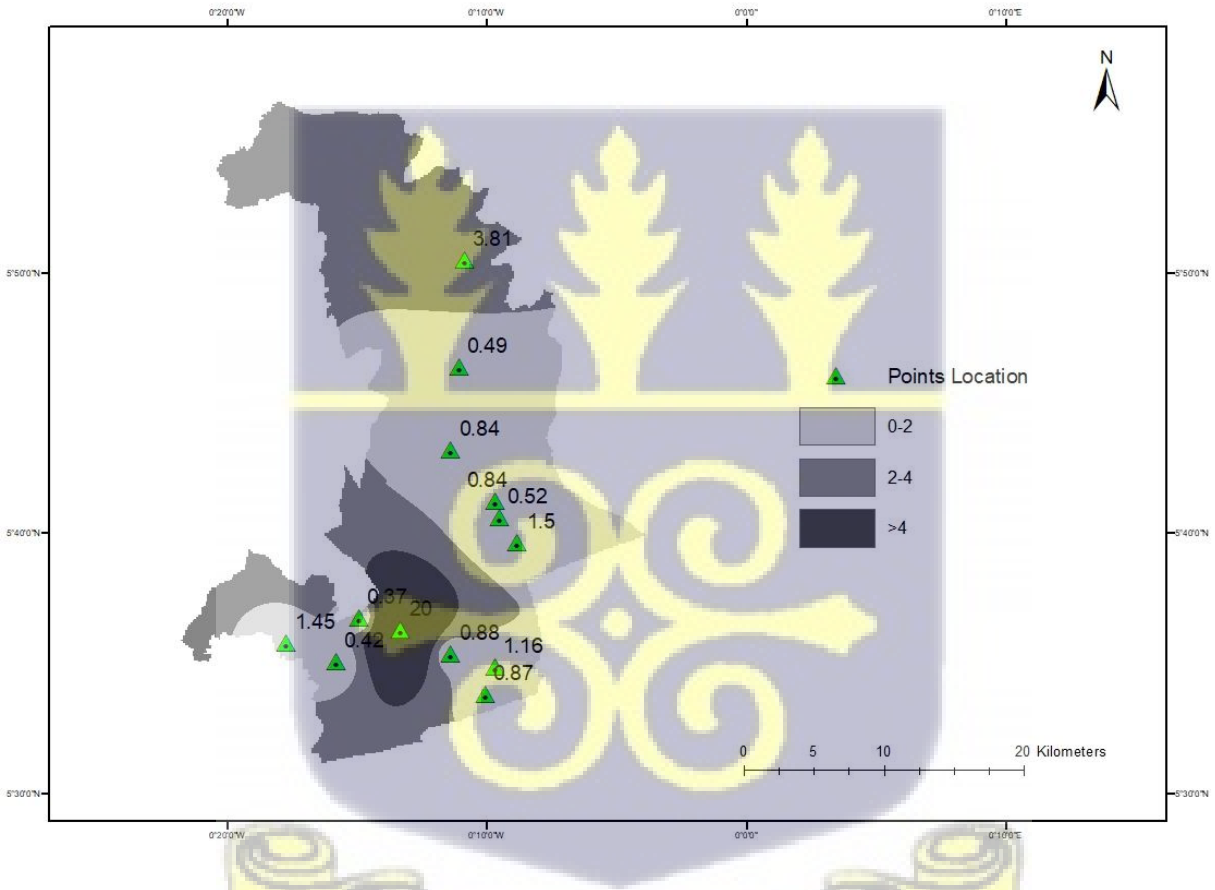

Figure 26 Interpolated map representing soil vulnerability index, Kg, for the study area

Zone 1 (grey) has the lowest vulnerability index values ranging from 0 – 2.0. Zone 2 has mostly intermediate vulnerability index values ranging from 2.0 – 4.0. Zone 3 (darker shade) has the highest vulnerability index values greater than 4.0 around the Tesano PS site. Areas in high soil

vulnerability index zones may need specific risk mitigation strategies such as soil stabilization techniques, deep foundation designs, or flexible building materials. Usually, in such areas, emergency management agencies prioritise earthquake preparedness drills, and public education campaigns among others.

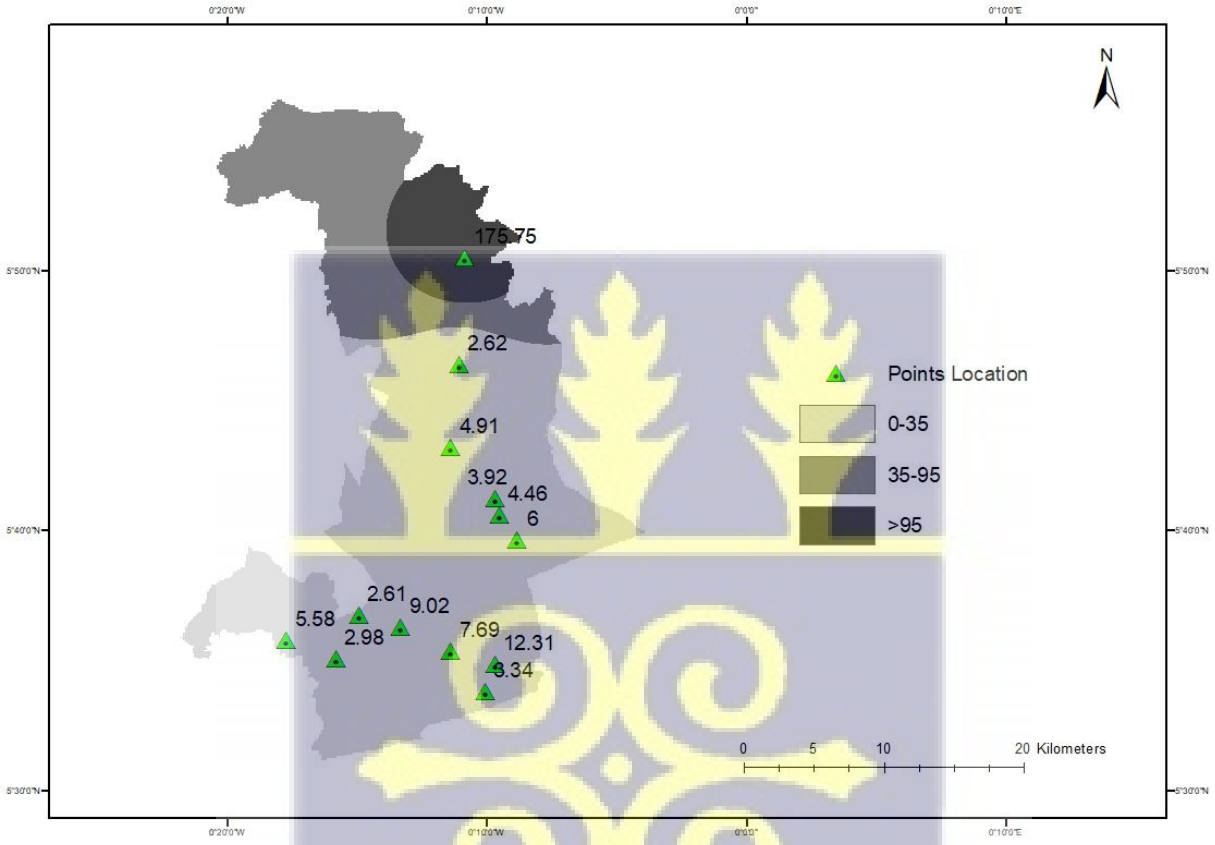

Figure 27 Interpolated Map representing sedimentary thickness, H, for the study area

.

Zone 1(grey) has the lowest sedimentary thickness values ranging from $0 - 35.0\ m$. Zone 2 has mostly intermediate sedimentary thickness values ranging from $35.0 - 95.0\ m$. Zone 3 (darker shade) has the highest sedimentary thickness values greater than $95.0\ m$. Generally, regions with thinner alluvium typically exhibit less amplification of seismic waves, as there is less

unconsolidated material to resonate with the seismic energy. Areas with thicker alluvial deposits are often associated with greater seismic wave amplification. This is because thicker, unconsolidated sediments tend to resonate more with seismic waves, potentially leading to higher ground motion.

CHAPTER FIVE

CONCLUSION AND RECOMMENDATIONS

The fundamental frequency, f_o, amplification factor, A_o, depth to bedrock H, and the vulnerability index K_g were estimated for 13 sites in the GAMA using the horizontal-to-vertical spectra ratio analysis of ambient noise. These estimates are important to understanding and assessing seismic risk in the study area. The interpretation of the H/V curve revealed four major patterns from the sites: clear single peaks, multiple peaks, and broad and flat peaks. The peaks correspond to major different seismic responses. The site in Aburi showed the smallest fundamental frequency and a flat curve indicating the least amplification to seismic waves. The site contains hard rock and is the least vulnerable among the sites. The vulnerability index estimation, however, indicates that is not the least vulnerable to liquefaction. Tesano PS revealed a single clear peak and the highest amplification factor indicating soft soils which are highly vulnerable to destruction than the other sites. The vulnerability index estimates are in clear agreement with this. There is evidence to support intuitive theories that higher seismic risk exists in areas where clay layers are present. The other sites can be classified as medium rocks comparing them to the ones at Tesano PS (soft) and Aburi (hard). They showed broad and multiple peaks which also inform about the seismic properties of the sites. Estimating such site effect parameters is the first essential stage in the mitigation of seismic hazards. To develop effective mitigation techniques to lessen the effects and reduce the damages caused by this natural hazard, policymakers and disaster management authorities will find the study's findings to be of great value. Clear peaks can therefore be used as an inference for seismic behavior and help inform engineering decisions to mitigate earthquake-related risk.

REFERENCES

Abdel-Rahman, K., Abd El-Aal, A. K., El-Hady, S. M., Mohamed, A. A., & Abdel-Moniem, E. (2012). Fundamental site frequency estimation at new domiat city, Egypt. *Arabian Journal of Geosciences*, *5*(4), 653–661. https://doi.org/10.1007/s12517-010-0222-2

Addae, B., & Oppelt, N. (2019). Land-Use/Land-Cover Change Analysis and Urban Growth Modelling in the Greater Accra Metropolitan Area (GAMA), Ghana. *Urban Science*, *3*(1). https://doi.org/10.3390/urbansci3010026

Adedini, S. A. (2022). Population dynamics, urbanisation and climate change in Africa's intermediate cities : what can family planning contribute ? 1–11.

Ahulu, S. T., Danuor, S. K., & Asiedu, D. K. (2018). Probabilistic seismic hazard assessment of southern part of Ghana, 539–557.

Akkaya, İ., & Özvan, A. (2019). Site characterization in the Van settlement (Eastern Turkey) using surface waves and HVSR microtremor methods. *Journal of Applied Geophysics*, *160*, 157–170. https://doi.org/10.1016/j.jappgeo.2018.11.009

Al-Halboosi, J. M., Mohammad, O. J., & Al-Heety, E. A. (2022). Seismicity of Iraqi western desert and surroundings: As an example of continental intraplate seismicity. *IOP Conference Series: Earth and Environmental Science*, *1080*(1), 012014. https://doi.org/10.1088/1755-1315/1080/1/012014

Allotey, N. K., Arku, G., & Amponsah, P. E. (2010). Earthquake-disaster preparedness: The case of Accra. *International Journal of Disaster Resilience in the Built Environment*, *1*(2), 140–156. https://doi.org/10.1108/17595901011056613

Amponsah, P. E. (2002). Seismic activity in relation to fault systems in southern Ghana. *Journal of African Earth Sciences*, *35*(2), 227–234. https://doi.org/10.1016/S0899-5362(02)00100-8

Amponsah, P. E. (2004). View of Seismic activity in Ghana_ past, present and future.pdf.

Amponsah, P. E., Banoeng-Yakubo, B. K., Panza, G. F., & Vaccari, F. (2009). Deterministic seismic ground modelling of the Greater Accra Metropolitan Area, Southeastern Ghana, *112*, 317–328. https://doi.org/10.2113/gssajg.112.3-4.317

Amponsah, P. E., Banoeng-Yakubo, B. K., Vaccari, F., & Panza, G. F. (2008). Seismic ground motion and hazard assessment of the Greater Accra Metropolitan Area, Southeastern Ghana.

Amponsah, P., Leydecker, G., & Muff, R. (2012). Earthquake catalogue of Ghana for the time period 1615-2003 with special reference to the tectono-structural evolution of south-east Ghana. *Journal of African Earth Sciences*, *75*, 1–13. https://doi.org/10.1016/j.jafrearsci.2012.07.002

Amponsah, P., Opoku-Ntim, I., & Nortey, G. (2020). Seismic risk in Ghana : efforts and challenges, 1–5.

Anastasopoulos, I., Gazetas, G., Bransby, M. F., Davies, M. C. R., & El Nahas, A. (2007). Fault Rupture Propagation through Sand: Finite-Element Analysis and Validation through Centrifuge Experiments. *Journal of Geotechnical and Geoenvironmental Engineering*, *133*(8), 943–958. https://doi.org/10.1061/(ASCE)1090-0241(2007)133:8(943)

Attoh, K., Brown, L., & Haenlein, J. (2005). The role of Pan-African structures in intraplate seismicity near the termination of the Romanche fracture zone, West Africa. *Journal of*

African Earth Sciences, *43*(5), 549–555. https://doi.org/10.1016/j.jafrearsci.2005.09.006

Ayetey, J. ., & Andoh, M. B. (1988). Earthquake Site Response Study of Accra Area, Ghana.

Bahavar, M., Spica, Z. J., Sánchez-Sesma, F. J., Trabant, C., Zandieh, A., & Toro, G. (2020). Horizontal-to-vertical spectral ratio (HVSR) IRIS station toolbox. *Seismological Research Letters*, *91*(6), 3539–3549. https://doi.org/10.1785/0220200047

Baker, J. W., Bradley, B A., and S. (2013). Introduction to Probabilistic Seismic Hazard Analysis.

Bard, P.-Y. (1994). Effects of surface geology on ground motion: Recent results and remaining issues. *Proceedings of 10Th European Conference on Earthquake Engineering*, (March), 305–323.

Bard, P. (1998). Microtremor measurement : a tool for site effect estimation? *K. Irikura K. Kudo H. Okada T. Sasatami Eds*, (August), 1251–1279.

Blundell, D. J. (1976). Active faults in West Africa. *Earth and Planetary Science Letters*, *31*(2), 287–290. https://doi.org/10.1016/0012-821X(76)90221-1

Bondesen, E., & Smit, A. F. J. (1972). Holocene Tectonic Activity in West Africa Dated by Archaeologic Methods: Discussion. *GSA Bulletin*, *83*(4), 1193–1196. https://doi.org/10.1130/0016-7606(1972)83[1193:HTAIWA]2.0.CO;2

Bonnefoy-Claudet, S., Baize, S., Bonilla, L. F., Berge-Thierry, C., Pasten, C., Campos, J., … Verdugo, R. (2009). Site effect evaluation in the basin of Santiago de Chile using ambient noise measurements. *Geophysical Journal International*, *176*(3), 925–937. https://doi.org/10.1111/j.1365-246X.2008.04020.x

Bonnefoy-Claudet, S., Cornou, C., Bard, P. Y., Cotton, F., Moczo, P., Kristek, J., & Fäh, D. (2006a). H/V ratio: A tool for site effects evaluation. Results from 1-D noise simulations. *Geophysical Journal International*, *167*(2), 827–837. https://doi.org/10.1111/j.1365-246X.2006.03154.x

Bonnefoy-Claudet, S., Cotton, F., & Bard, P. Y. (2006b). The nature of noise wavefield and its applications for site effects studies. A literature review. *Earth-Science Reviews*, *79*(3–4), 205–227. https://doi.org/10.1016/j.earscirev.2006.07.004

Bour, M., Fouissac, D., Dominique, P., & Martin, C. (1998). On the use of microtremor recordings in seismic microzonation. *Soil Dynamics and Earthquake Engineering*, *17*(7–8), 465–474. https://doi.org/10.1016/S0267-7261(98)00014-1

Bray, J. D. (2009). Designing buildings to accommodate earthquake surface fault rupture. In *Improving the Seismic Performance of Existing Buildings and Other Structures - Proc. 2009 ATC and SEI Conference on Improving the Seismic Performance of Existing Buildings and Other Structures* (pp. 1269–1280). https://doi.org/10.1061/41084(364)117

Brown, L. T., Diehl, J. G., & Nigbor, R. L. (2000). A Simplified Procedure To Measure Average Shear-Wave Velocity To a Depth of 30 Meters (Vs30). *12Wcee*, 1–8. Retrieved from http://www.iitk.ac.in/nicee/wcee/article/0677.pdf

Cadet, H., Macau, A., Benjumea, B., Bellmunt, F., & Figueras, S. (2011). From ambient noise recordings to site effect assessment: The case study of Barcelona microzonation. *Soil Dynamics and Earthquake Engineering*, *31*(3), 271–281. https://doi.org/10.1016/j.soildyn.2010.07.005

Camelbeeck, T., Van Noten, K., Lecocq, T., & Hendrickx, M. (2022). The damaging character of

shallow 20th-century earthquakes in the Hainaut coal area (Belgium). *Solid Earth*, *13*(3), 469–495. https://doi.org/10.5194/se-13-469-2022

Campbell, G., Lubkowski, Z., Villani, M., & Polidoro, B. (2018). A Seismic Source Model for West Africa, (June), 1–13. Retrieved from https://www.researchgate.net/publication/325988747

Castellaro, S., & Mulargia, F. (2009). VS30 estimates using constrained H/V measurements. *Bulletin of the Seismological Society of America*, *99*(2 A), 761–773. https://doi.org/10.1785/0120080179

Chatelain, J. L., & Guillier, B. (2013). Reliable fundamental frequencies of soils and buildings down to 0.1 Hz obtained from ambient vibration recordings with a 4.5-Hz sensor. *Seismological Research Letters*, *84*(2), 199–209. https://doi.org/10.1785/0220120003

Chen, Q. F., Liu, L. B., Wang, W. J., & Rohrbach, E. (2009). Site effects on earthquake ground motion based on microtremor measurements for metropolitan Beijing. *Chinese Science Bulletin*, *54*(2), 280–287. https://doi.org/10.1007/s11434-008-0422-2

Chen, Y., Song, J., Zhong, S., Liu, Z., & Gao, W. (2021). Effect of destructive earthquake on the population-economy-space urbanization at the county level. A Case Study on Dujiangyan County, China. *Sustainable Cities and Society*, 103345. https://doi.org/10.1016/j.scs.2021.103345

Craig, T. J., Jackson, J. A., Priestley, K., & Mckenzie, D. (2011). Earthquake distribution patterns in Africa: Their relationship to variations in lithospheric and geological structure, and their rheological implications. *Geophysical Journal International*, *185*(1), 403–434. https://doi.org/10.1111/j.1365-246X.2011.04950.x

Cruz, E., Riddell, R., & Midorikawa, S. (1993). A study of site amplification effects on ground motions in Santiago, Chile. *Tectonophysics*, *218*(1–3), 273–280. https://doi.org/10.1016/0040-1951(93)90273-M

D'Amico, V., Picozzi, M., Baliva, F., & Albarello, D. (2008). Ambient noise measurements for preliminary site-effects characterization in the Urban area of Florence, Italy. *Bulletin of the Seismological Society of America*, *98*(3), 1373–1388. https://doi.org/10.1785/0120070231

Damayanti, C., & Sismanto, S. (2021). The Relationship Between Amplification And Quality Factors of Seismic Waves In Surface Sediment Layer, 2–7. https://doi.org/10.4108/eai.30-8-2021.2311500

Dawood, A. M. A., Akiti, T. T., & Glover, E. T. (2012). Seismic Refraction Investigation at a Radioactive Waste Disposal Site. *Journal of Geo-Sciences*, *2*(2), 7–13. https://doi.org/10.5923/j.geo.20120202.02

De Guevara, J. L., Mojica, A., Ruíz, A., Ho, C. A., Rodríguez, K., Toral, J., & Fábrega, J. (2022). Ambient Noise H/V Spectral Ratio in Site Effect Estimation in La Mesa de Macaracas, Panama. *International Journal of Geophysics*, *2022*. https://doi.org/10.1155/2022/6171529

Devendran, A. A., & Banon, F. (2022). Spatio-Temporal Land Cover Analysis and the Impact of Land Cover Variability Indices on Land Surface Temperature in Greater Accra, Ghana Using Multi-Temporal Landsat Data, *14*, 240–258. https://doi.org/10.4236/jgis.2022.143013

Dikmen, S. U., Edincliler, A., & Pinar, A. (2015). Northern Aegean Earthquake (Mw=6.9): Observations at three seismic downhole arrays in Istanbul. *Soil Dynamics and Earthquake*

Engineering, *77*, 321–336. https://doi.org/10.1016/j.soildyn.2015.06.008

Doglioni, C. (2018). A classification of induced seismicity. *Geoscience Frontiers*, *9*(6), 1903–1909. https://doi.org/10.1016/j.gsf.2017.11.015

Fäh, D., Rüttener, E., Noack, T., & Kruspan, P. (1997). Microzonation of the city of Basel. *Journal of Seismology*, *1*(1), 87–102. https://doi.org/10.1023/A:1009774423900

Fairhead, J. D., & Girdler, R. W. (1971). The Seismicity of Africa. *Geophysical Journal of the Royal Astronomical Society*, *24*(3), 271–301. https://doi.org/10.1111/j.1365-246X.1971.tb02178.x

Field, E., & Jacob, K. (1993). The theoretical response of sedimentary layers to ambient seismic noise. *October*, *20*(24), 2925–2928.

Forte, G., Chioccarelli, E., De Falco, M., Cito, P., Santo, A., & Iervolino, I. (2019). Seismic soil classification of Italy based on surface geology and shear-wave velocity measurements. *Soil Dynamics and Earthquake Engineering*, *122*(October 2018), 79–93. https://doi.org/10.1016/j.soildyn.2019.04.002

Foulger, G. R., Wilson, M., Gluyas, J., Julian, B. R., & Davies, R. (2017). Global Review of Human-Induced Earthquakes. *Earth-Science Reviews*. https://doi.org/10.1016/j.earscirev.2017.07.008

Giardini, D., Grunthal, G., Shedlock, K. M., & Zhang, P. (1999). The GSHAP Global Seismic Hazard Map. ANNALI DI GEOFISICA.

Gospe, T., Zimmaro, P., Wang, P., Buckreis, T., Ahdi, S. K., Yong, A. K., … Stewart, J. P. (2020). Supplementing Shear Wave Velocity Profile Database With Microtremor-Based H /

V Spectral Ratios, *003010*(Abstract ID), 1–13.

Grigoli, F., Cesca, S., Priolo, E., Rinaldi, A. P., Clinton, J. F., Stabile, T. A., … Dahm, T. (2017). Current challenges in monitoring, discrimination, and management of induced seismicity related to underground industrial activities: A European perspective. *Reviews of Geophysics*, *55*(2), 310–340. https://doi.org/10.1002/2016RG000542

Guéguen, P., Chatelain, J. L., Guillier, B., & Yepes, H. (2000). An indication of the soil topmost layer response in Quito (Ecuador) using noise H/V spectral ratio. *Soil Dynamics and Earthquake Engineering*, *19*(2), 127–133. https://doi.org/10.1016/S0267-7261(99)00035-4

Gurler, E. D., Nakamura, Y., Saita, J., & Sato, T. (2000). Local site effect of Mexico City based on microtremor measurement. *International Conference on Seismic Zonation. Palm Spring Riviera Resort, California, USA*, 65.

Gyau-Boakye, P., Kankam-Yeboah, K., Darko, P. K., Dapaah-Siakwan, S., & Duah, A. A. (2008). Groundwater as a vital resource for rural development: An example from Ghana. In *Applied Groundwater Studies in Africa* (Vol. 70, pp. 149–170). https://doi.org/10.1201/9780203889497-12

Horike, M. (1985). Inversion of phase velocity of long-period microtremors to the S-wave-velocity structure down to the basement in urbanized areas. *Journal of Physics of the Earth*, *33*(2), 59–96. https://doi.org/10.4294/jpe1952.33.59

Huang, H. C., & Tseng, Y. S. (2002). Characteristics of soil liquefaction using H/V of microtremors in Yuan-Lin area, Taiwan. *Terrestrial, Atmospheric and Oceanic Sciences*, *13*(3), 325–338. https://doi.org/10.3319/TAO.2002.13.3.325(CCE)

Hunter, J. A., Benjumea, B., Harris, J. B., Miller, R. D., Pullan, S. E., Burns, R. A., & Good, R. L. (2002). Surface and downhole shear wave seismic methods for thick soil site investigations q. *Soil Dynamics and Earthquake Engineering*, *22*(9–12), 931–941. https://doi.org/10.1016/S0267-7261(02)00117-3

Imoro Musah, B., Peng, L., & Xu, Y. (2020). Urban Congestion and Pollution: A Quest for Cogent Solutions for Accra City. In *IOP Conference Series: Earth and Environmental Science* (Vol. 435). https://doi.org/10.1088/1755-1315/435/1/012026

Irinyemi, S. A., Lombardi, D., & Ahmad, S. M. (2022). Probabilistic seismic hazard assessment for West Africa region. *Georisk*, *16*(2), 315–329. https://doi.org/10.1080/17499518.2021.1952608

Janusz, P., Perron, V., Knellwolf, C., & Fäh, D. (2022). Combining Earthquake Ground Motion and Ambient Vibration Recordings to Evaluate a Local High-Resolution Amplification Model—Insight From the Lucerne Area, Switzerland. *Frontiers in Earth Science*, *10*(May), 1–19. https://doi.org/10.3389/feart.2022.885724

Johnson, C. D., & Lane, J. W. (2016). Statistical comparison of methods for estimating sediment thickness from horizontal-to-vertical spectral ratio (HVSR) seismic methods: An example from Tylerville, Connecticut, USA. *Proceedings of the Symposium on the Application of Geophysics to Engineering and Environmental Problems, SAGEEP*, *2016-Janua*(2006). https://doi.org/10.4133/sageep.29-057

Junner, N.. (1941). The Accra earthquake of June 22, 1939. *Gold Coast Geological Survey*, *147*(3737), 751–752. https://doi.org/10.1038/147751a0

Kadiri, A. U., & Kijko, A. (2021). Seismicity and seismic hazard assessment in West Africa.

Journal of African Earth Sciences, *183*(March), 104305. https://doi.org/10.1016/j.jafrearsci.2021.104305

Kadiri, U. A., & Amponsah, P. E. (2021). Computation of area-characteristic seismicity parameters in Ghana, Nigeria, and immediate neighbours. *Arabian Journal of Geosciences*, *14*(13). https://doi.org/10.1007/s12517-021-07558-6

Komacek, T. D., López-ballesteros, A., Beck, J., & Bombelli, A. (2017). Urbanization in Africa : challenges and opportunities for conservation OPEN ACCESS Urbanization in Africa : challenges and opportunities for conservation. *Environ. Res. Lett*, (015002), 2–9. Retrieved from https://doi.org/10.1088/1748-9326/aa94fe

Konno, K., & Ohmachi, T. (1998). Ground-motion characteristics estimated from spectral ratio between horizontal and vertical components of microtremor. *Bulletin of the Seismological Society of America*, *88*(1), 228–241. https://doi.org/10.1785/bssa0880010228

Krinitzsky, E. L. (1995). Deterministic versus probabilistic seismic hazard analysis for critical structures. *Engineering Geology*, *40*(1–2), 1–7. https://doi.org/10.1016/0013-7952(95)00031-3

Kutu, J. M. (2013). Seismic and Tectonic Correspondence of Major Earthquake Regions in Southern Ghana with Mid-Atlantic Transform-Fracture Zones. *International Journal of Geosciences*, *04*(10), 1326–1332. https://doi.org/10.4236/ijg.2013.410128

Leite Neto, G. da S., & Julià, J. (2022). Determination of Intraplate Focal Mechanisms with the Brazilian Seismic Network: A Simplified Cut-and-Paste Approach. *SSRN Electronic Journal*, *121*(December 2022). https://doi.org/10.2139/ssrn.4214555

Lermo, J., & Chavez-Garcia, J. F. (1993). Site effect evaluation using spectral ratios with only one station. *Bulletin of the Seismological Society of America*, *83*(October 1993), 1574–1594.

Leyton, F., Ruiz, J., Campos, J., & Kausel, E. (2009). Intraplate and interplate earthquakes in Chilean subduction zone: A theoretical and observational comparison. *Physics of the Earth and Planetary Interiors*, *175*(1–2), 37–46. https://doi.org/10.1016/j.pepi.2008.03.017

Liu, L., Chen, Q. F., Wang, W., & Rohrbach, E. (2014). Ambient noise as the new source for urban engineering seismology and earthquake engineering: A case study from Beijing metropolitan area. *Earthquake Science*, *27*(1), 89–100. https://doi.org/10.1007/s11589-013-0052-x

Marcellini, A. (2006). Guidelines for the Implementation of the H / V Spectral Ratio Technique on Ambient Vibrations. *Interpretation A Journal Of Bible And Theology*, (March), 1–69. Retrieved from http://sesame-fp5.obs.ujf-grenoble.fr

Meghraoui, M., Amponsah, P., Ayadi, A., Ayele, A., Ateba, B., Bensuleman, A., … Strasbourg, I. P. G. (2016). The Seismotectonic Map of Africa. *Episodes*, *39*(1), 1–10. https://doi.org/10.18814/epiiugs/2016/v39i1/89232

Meghraoui, M., Amponsah, P., Bernard, P., & Ateba, B. (2019). Active transform faults in the Gulf of Guinea : insights from geophysical data and implications for seismic hazard assessment 1, *1408*(May), 1398–1408.

Molnar, S., Cassidy, J. F., Monahan, P. A., & Dosso, S. E. (2007a). Comparison of Geophysical Shear-Wave Velocity Methods. *Ninth Canadian Conference on Earthquake Engineering*, (June), 390–400.

Molnar, S., Cassidy, J. F., Monahan, P. A., Onur, T., Ventura, C., & Rosenberger, A. (2007b). Earthquake Site Response Studies Using Microtremor Measurements in Southwestern British Columbia. *Ninth Canadian Conference on Earthquake Engineering*, (June), 410–419.

Moustafa, S. S. R., Abdalzaher, M. S., Naeem, M., & Fouda, M. M. (2022). Seismic Hazard and Site Suitability Evaluation Based on Multicriteria Decision Analysis. *IEEE Access*, *10*(June), 69511–69530. https://doi.org/10.1109/ACCESS.2022.3186937

Mulargia, F., & Castellaro, S. (2016). HVSR deep mapping tested down to ~1.8 km in Po Plane Valley, Italy. *Physics of the Earth and Planetary Interiors*, *261*, 17–23. https://doi.org/10.1016/j.pepi.2016.08.002

Mundepi, A. K., Galiana-Merino, J. J., Asthana, A. K. L., & Rosa-Cintas, S. (2015). Soil characteristics in Doon Valley (northwest Himalaya, India) by inversion of H/V spectral ratios from ambient noise measurements. *Soil Dynamics and Earthquake Engineering*, *77*, 309–320. https://doi.org/10.1016/j.soildyn.2015.06.006

Murbach, D., Rockwell, T. K., & Bray, J. D. (1999). The Relationship of Foundation Deformation to Surface and Near-Surface Faulting Resulting from the 1992 Landers Earthquake. *Earthquake Spectra*, *15*(1), 121–144. https://doi.org/10.1193/1.1586032

Nakamura, Y. (1996). Real-time information systems for hazard mitigation. *In Proceedings of the 11th World Conference on Earthquake Engineering*, 23–28.

Nakamura, Y. (1997). Seismic vulnerability indices for ground and structures using microtremor. *World Congress on Railway Research*, 1–7.

Nakamura, Y. (2000). Clear Identification of Fundamental Idea of Nakamura ' S. *Spectrum*, 2656.

Nakamura, Y. (2019). What is the Nakamura method? *Seismological Research Letters*, *90*(4), 1437–1443. https://doi.org/10.1785/0220180376

Nakamura, Y., Sato, T., & Nishinaga, M. (2000). Local Site Effect of Kobe Based on Microtremor. *Proceedings of the Sixth International Conference on Seismic Zonation (6ISCZ) EERI, November 12-15, 2000/ Palm Springs. California*, (April), 3–8.

Nappi, R., Porfido, S., Paganini, E., Vezzoli, L., Ferrario, M. F., Gaudiosi, G., … Michetti, A. M. (2021). The 2017, md = 4.0, casamicciola earthquake: Esi-07 scale evaluation and implications for the source model. *Geosciences (Switzerland)*, *11*(2), 1–16. https://doi.org/10.3390/geosciences11020044

Nicol, A., Carne, R., Gerstenberger, M., & Christophersen, A. (2011). Induced seismicity and its implications for CO2 storage risk. *Energy Procedia*, *4*, 3699–3706. https://doi.org/10.1016/j.egypro.2011.02.302

Nievas, C. I., Bommer, J. J., Crowley, H., van Elk, J., Ntinalexis, M., & Sangirardi, M. (2020). A database of damaging small-to-medium magnitude earthquakes. *Journal of Seismology*, *24*(2), 263–292. https://doi.org/10.1007/s10950-019-09897-0

Nortey, G., Armah, T. K., & Amponsah, P. (2018). Vs30 mapping at selected sites within the Greater Accra Metropolitan Area. *Journal of African Earth Sciences*, *142*, 158–169. https://doi.org/10.1016/j.jafrearsci.2018.02.020

Oettle, N. K., & Bray, J. D. (2013). Geotechnical Mitigation Strategies for Earthquake Surface

Fault Rupture. *Journal of Geotechnical and Geoenvironmental Engineering*, *139*(11), 1864–1874. https://doi.org/10.1061/(ASCE)gt.1943-5606.0000933

Onyebueke, E., Durrheim, R., & Manzi, M. (2017). Assessment of Site Effect at the Seismological Stations in South Africa Using the HVSR Technique Assessment of Site Effect at the Seismological Stations in South Africa Using the HVSR Technique, (September).

Osei, J. B., Adom-Asamoah, M., Awadallah Ahmed, A. A., & Antwi, E. B. (2018). Monte Carlo Based Seismic Hazard Model for Southern Ghana. *Civil Engineering Journal*, *4*(7), 1510. https://doi.org/10.28991/cej-0309191

Owusu, G. (2012). Coping with Urban Sprawl: A Critical Discussion of the Urban Containment Strategy in a Developing Country City, Accra. *The Journal of Urbanism*, *2*, 17.

Panza, G. F., Romanelli, F., & Vaccari, F. (2001). Seismic wave propagation in laterally heterogeneous anelastic media Vol. 43. *Advances in Geophysics, Volume 43*, 1–95. Retrieved from http://www.sciencedirect.com/science/article/B7RNH-4NDG0D8-2/2/d526b2aa840d0ce093f69387b591ccce

Parolai, S. (2012). Investigation of Site Responses in Urban Areas by Using Earthquake Data and Seismic Noise. *New Manual of Seismological Observatory Practice 2*, (January), 1–41. https://doi.org/10.2312/GFZ.NMSOP-2

Parolai, S., Richwalski, S. M., Milkereit, C., & Bormann, P. (2004). Assessment of the stability of H/V spectral ratios from ambient noise and comparison with earthquake data in the Cologne area (Germany). *Tectonophysics*, *390*(1–4), 57–73. https://doi.org/10.1016/j.tecto.2004.03.024

Paudyal, Y. R., Yatabe, R., Bhandary, N. P., & Dahal, R. K. (2012). A study of local amplification effect of soil layers on ground motion in the Kathmandu Valley using microtremor analysis. *Earthquake Engineering and Engineering Dynamics*, *11*(2), 257–268. https://doi.org/10.1007/s11803-012-0115-3

Piña-Flores, J., Cárdenas-Soto, M., García-Jerez, A., Seivane, H., Luzón, F., & Sánchez-Sesma, F. J. (2020). Use of peaks and troughs in the horizontal-to-vertical spectral ratio of ambient noise for Rayleigh-wave dispersion curve picking. *Journal of Applied Geophysics*, *177*. https://doi.org/10.1016/j.jappgeo.2020.104024

Pitilakis, K., Riga, E., Anastasiadis, A., Fotopoulou, S., & Karafagka, S. (2019). Towards the revision of EC8: Proposal for an alternative site classification scheme and associated intensity-dependent spectral amplification factors. *Soil Dynamics and Earthquake Engineering*, *126*(March), 105137. https://doi.org/10.1016/j.soildyn.2018.03.030

Quaah, A. O. (1982). A study of past major earthquakes in southern Ghana using intensity data. *Tectonophysics*, *88*(1–2), 175–188. https://doi.org/10.1016/0040-1951(82)90208-6

Ranjan, R. (2005). Seismic Response Analysis of Dehradun. *International Institute for Geo-Information Science and Earth Observations–Enschede, Netherlands*.

Rošer, J., & Gosar, A. (2010). Determination of Vs30 for seismic ground classification in the Ljubljana area, Slovenia. *Acta Geotechnica Slovenica*, *7*(1), 61–76.

Rubinstein, J. L., & Mahani, A. B. (2015). Myths and facts on wastewater injection, hydraulic fracturing, enhanced oil recovery, and induced seismicity. *Seismological Research Letters*, *86*(4), 1060–1067. https://doi.org/10.1785/0220150067

Seht, M. I. Von, & Wohlenberg, J. (1999). Microtremor Measurements Used to Map Thickness of Soft Sediments. *Bulletin of the Seismological Society of America*, *89*(1), 250–259. https://doi.org/10.1785/bssa0890010250

Sens-Schönfelder, C., & Brenguier, F. (2019). Chapter 9: Noise-based monitoring. *Seismic Ambient Noise*, 267–301.

SESAME (Site EffectS Assessment using AMbient Excitations). (2004). Guidelines for the implementation of the H/V spectral ratio technique on ambient vibration measurements, processing and interpretation. Sesame project-Deliverable D23. 12-WP12-, (December).

Shatkay, H. (1995). The Fourier Transform - A Primer. *Department of Computer Science Brown University Providence, Rhode Island 02912*, (November), 18.

Stehly, L., Campillo, M., & Shapiro, N. M. (2006). A study of the seismic noise from its long-range correlation properties. *Journal of Geophysical Research: Solid Earth*, *111*(10), 1–12. https://doi.org/10.1029/2005JB004237

Stow, D. A., Weeks, J. R., Shih, H. C., Coulter, L. L., Johnson, H., Tsai, Y. H., … Mensah, F. (2016). Inter-regional pattern of urbanization in southern Ghana in the first decade of the new millennium. *Applied Geography*, *71*, 32–43. https://doi.org/10.1016/j.apgeog.2016.04.006

Suhendra, Zul Bahrum, C., & Sugianto, N. (2018). Geological condition at landslides potential area based on microtremor survey. *ARPN Journal of Engineering and Applied Sciences*, *13*(8), 3007–3013.

Sykes, L. R. (1978). Intraplate seismicity, reactivation of preexisting zones of weakness, alkaline

magmatism, and other tectonism postdating continental fragmentation. *Reviews of Geophysics*. https://doi.org/10.1029/RG016i004p00621

Talha Qadri, S. M., Nawaz, B., Sajjad, S. H., & Sheikh, R. A. (2015). Ambient noise H/V spectral ratio in site effects estimation in Fateh Jang area, Pakistan. *Earthquake Science*, *28*(1), 87–95. https://doi.org/10.1007/s11589-014-0105-9

Tanjung, N. A. F., Permatasari, I., & Yuniarto, A. H. P. (2021). Mapping of weathered layer thickness and Seismic Vulnerability in Tegal using the HVSR method. *Journal of Physics: Conference Series*, *1951*(1). https://doi.org/10.1088/1742-6596/1951/1/012053

Teague, D. P., Cox, B. R., & Rathje, E. M. (2018). Measured vs. predicted site response at the Garner Valley Downhole Array considering shear wave velocity uncertainty from borehole and surface wave methods. *Soil Dynamics and Earthquake Engineering*, *113*(May), 339–355. https://doi.org/10.1016/j.soildyn.2018.05.031

Tian, B., Du, Y., You, Z., & Zhang, R. (2019). Measuring the sediment thickness in urban areas using the revised H/V spectral ratio method. *Engineering Geology*, *260*(July), 105223. https://doi.org/10.1016/j.enggeo.2019.105223

Ullah, I., & Prado, R. L. (2017). Soft sediment thickness and shear-wave velocity estimation from the H/V technique up to the bedrock at meteorite impact crater site, Sao Paulo city, Brazil. *Soil Dynamics and Earthquake Engineering*, *94*(February 2016), 215–222. https://doi.org/10.1016/j.soildyn.2017.01.015

Van Ginkel, J., Ruigrok, E., Stafleu, J., & Herber, R. (2022). Development of a seismic site-response zonation map for the Netherlands. *Natural Hazards and Earth System Sciences*, *22*(1), 41–63. https://doi.org/10.5194/nhess-22-41-2022

Vella, A., Galea, P., & D'Amico, S. (2013). Site frequency response characterisation of the Maltese islands based on ambient noise H/V ratios. *Engineering Geology*, *163*, 89–100. https://doi.org/10.1016/j.enggeo.2013.06.006

Wathelet, M., Chatelain, J. L., Cornou, C., Giulio, G. Di, Guillier, B., Ohrnberger, M., & Savvaidis, A. (2020). Geopsy: A user-friendly open-source tool set for ambient vibration processing. *Seismological Research Letters*, *91*(3), 1878–1889. https://doi.org/10.1785/0220190360

Yang, Y., & Ritzwoller, M. H. (2008). Characteristics of ambient seismic noise as a source for surface wave tomography. *Geochemistry, Geophysics, Geosystems*, *9*(2). https://doi.org/10.1029/2007GC001814